Preclinical and clinical biomarker studies of CT181

Preclinical and clinical biomarker studies of CT1812: a novel approach to Alzheimer's disease modification

Nicholas J. Izzo[1], Carla M. Yuede[2], Kelsie M. LaBarbera[1], Colleen S. Limegrover[1], Courtney Rehak[1], Raymond Yurko[1], Lora Waybright,[1] Gary Look[1], Gilbert Rishton[1], Hank Safferstein[1], Mary E. Hamby[1], Claire Williams[1], Kelsey Sadlek[1], Hannah M. Edwards[2], Chuck Davis[3], Michael Grundman[4,5], Lon S. Schneider[6], Steven T. DeKosky[7], Daniel Chelsky[8], Ian Pike[9], Christopher Henstridge[10], Kaj Blennow[11,12], Henrik Zetterberg[11,12,13], Harry LeVine III[14], Tara L. Spires-Jones[15], John R. Cirrito[2], Susan M. Catalano[1*]

[1]Cognition Therapeutics Inc., Pittsburgh, PA, USA
[2]Washington University, St. Louis, MO, USA
[3]CSD Biostatistics Inc., San Diego, CA, USA
[4] Global R&D Partners, San Diego, CA, USA
[5]University of California San Diego, San Diego, CA, USA
[6]Keck School of Medicine of USC, Los Angeles, CA, USA
[7]McKnight Brain Institute, University of Florida, Gainesville, FL, USA
[8]Caprion Biosciences, Montreal, QC, Canada
[9]Proteome Sciences, London, UK
[10] University of Dundee School of Medicine, Dundee, UK
[11]University of Gothenburg, Mölndal, Sweden
[12]Sahlgrenska University Hospital, Mölndal, Sweden
[13]UCL Institute of Neurology, London, UK
[14]Sanders-Brown Center on Aging, University of Kentucky, KY, USA
[15]The University of Edinburgh, Edinburgh, UK

*To whom correspondence should be addressed: Susan Catalano, Ph.D., Cognition Therapeutics Inc., 2403 Sidney Street, Suite 261, Pittsburgh, PA 15203 (scatalano@cogrx.com)

Abstract: CT1812 is an orally bioavailable, brain penetrant small molecule antagonist of the sigma-2 receptor complex with a novel disease-modifying mechanism of action against Alzheimer's disease (AD). Amyloid beta (Aβ) oligomers are one of the most toxic structural forms of the Aβ protein and are hypothesized to cause synaptotoxicity and memory failure as they build up in Alzheimer's patients' brain tissue. CT1812 displaced Aβ oligomers bound to synaptic receptors in three independent preclinical models of AD, facilitated oligomer clearance into the CSF, increased synaptic number and protein expression in neurons, and improved cognitive performance in transgenic mice. In a phase 1b/2a clinical trial, CT1812 increased CSF concentrations of Aβ oligomers, reduced concentrations of synaptic proteins and phosphorylated tau fragments, and reversed expression of many of the AD-related proteins dysregulated in CSF when administered to mild to moderate AD patients once daily for 28 days. These results are consistent with preclinical data and provide evidence of target engagement and impact on fundamental disease-related signaling pathways in AD patients, supporting further development of CT1812.

Introduction

Alzheimer's disease (AD) afflicts six million people in the US, yet disease modifying therapies remain an unmet medical need. Investigational therapeutics are directed against a variety of potential targets [1] but the amyloid hypothesis remains a compelling rationale for AD drug development [2]. More than 200 human mutations that cause early-onset familial AD have been identified, almost all conferring a single phenotype, increased Aβ protein concentration or ratio [3,4]. The only protective mutation that both significantly lowers AD incidence and also exhibits strong functional evidence of protection, A673T (the Icelandic mutation), also impacts the Aβ protein [5] resulting in significantly lowered binding affinity of Aβ oligomers at synaptic receptors [6]. Previous therapeutics have not effectively targeted amyloid beta (Aβ) oligomers [7], one of the most toxic structural forms of the Aβ protein [8]. While monomeric Aβ binds to many receptors, the oligomeric form of Aβ has been shown to bind specifically and saturably to a single receptor site composed of LilRB2, Nogo receptor, and cellular prion proteins [9–11] on neuronal synapses, where they induce changes consistent with a toxic disease-related ligand. Following oligomer binding, synaptic protein expression and the number of spines and synapses are reduced [12–16], synaptic plasticity processes (long term potential and depression) are disrupted [14,17–25] and the process of new memory formation fails [2,8,10,11,26]. Importantly, many preclinical studies suggest that following removal or reduction of the toxic oligomer species, synaptic protein expression, synapse number, and behavioral deficits can recover to normal levels [12,27].

Here we report the discovery and continued development of drug candidate CT1812, a brain penetrant small molecule that targets Aβ oligomers via a novel mechanism [26,28]. The first selective sigma-2 receptor antagonist to reach clinical trials [29], CT1812 is shown here to specifically displace Aβ oligomers bound to neuronal receptors at synapses without affecting monomer concentration. The sigma-2 receptor complex plays a major role in cellular damage response mechanisms, with its constituent proteins regulating processes as diverse as autophagy, cholesterol synthesis and progesterone signaling, lipid membrane-bound protein trafficking and receptor stabilization at the cell surface [30–37]. The sigma-2 receptor complex has been previously shown to be a key regulator of Aβ oligomer receptors [26,28]. In the present study, we demonstrate that when CT1812 binds specifically to the sigma-2 receptor ligand binding site and allosterically modulates the sigma-2 receptor complex, it causes destabilization of the neighboring Aβ oligomer receptor binding sites, resulting in displacement of Aβ oligomers from their receptors (in other words, an increase in their "off rate"). This lowers Aβ oligomer affinity for synaptic receptors, which phenocopies the effect of the protective Icelandic mutation. This disruption of oligomer binding has previously been associated with an improvement in membrane trafficking, neuronal surface expression of synaptic proteins, prevention of spine loss, and improvement in cognitive deficits in animal models of AD [26,28].

The present study additionally reports preclinical data demonstrating the novel mechanism of action of CT1812 in vitro and in vivo in an AD transgenic mouse model that highlights its potential therapeutic value and preliminary CSF biomarker data from the completed phase 1b/2a trial (NCT02907567), supporting its disease-modifying mechanism in AD patients [29].

Results

CT1812 displaces and prevents Aβ oligomer binding

Previously published studies that described unbiased proprietary library screening to identify compounds that block Aβ oligomer-induced toxicity of intracellular lipid membrane trafficking rates revealed compound potency correlated with sigma-2 receptor affinity [26,28]. Medicinal chemistry optimization resulted in the design of CT1812. CT1812 binds sigma-2 receptors with high affinity (Fig. 1A, Ki = 8.5 nM), sigma-1 receptors with low affinity (Ki = 63 nM), and is 100-fold selective for interacting with sigma-2 receptors vs. 72 other drug targets (Cerep/Eurofins Supplementary Fig. S1). CT1812 effectively prevented (EC50 = 6.7 μM) and reversed (EC50 = 0.36 μM) synthetic Aβ oligomer-induced membrane trafficking deficits in vitro in primary hippocampal/cortical cultures (21DIV, Fig. 1B) and prevented human AD patient brain-derived oligomer-induced trafficking deficits (Fig 1C). CT1812 prevented binding of Aβ oligomers to synaptic receptor sites on neurons (Aβ oligomer binding Kd = 0.43 μM, plus CT1812 = 1.12 μM, Fig. 2A, B, D), and also displaced already-bound Aβ oligomers (Aβ oligomer binding Kd = 0.61 μM, plus CT1812 = 1.16 μM, Fig. 2C, E). CT1812 did not block the formation of Aβ oligomers or disrupt their formation at concentrations up to 20μM (Supplementary Fig. S2), suggesting that its ability to stop Aβ oligomer binding and trafficking deficits results from CT1812 direct binding to sigma-2 receptors.

CT1812 restores disease-related protein expression and synapse number in vitro

Aβ oligomers induce reversible spine retraction in vitro [38] and cause a corresponding loss of synapses and synaptic proteins [13,26]. The effect of CT1812-induced displacement of Aβ oligomers on oligomer-induced spine and synapse loss in cultured rat neurons was investigated using the cytoskeleton binding protein drebrin (expressed postsynaptically) as a marker of synapse number. Addition of Aβ oligomers to neuronal cultures for 3 hours caused a significant loss (mean ± SEM 12.8% ± 2.6%, $p < 0.01$, 2-tailed Students t-test, Fig. 2F top, G) of drebrin-immunoreactive synaptic puncta per neuron compared to vehicle treatment. This is similar to the degree of synapse loss seen using ultrastructural stereology methods in postmortem hippocampus from humans diagnosed with mild cognitive impairment [39]. CT1812 prevented oligomer-induced synapse loss in a dose-dependent manner (EC50 = 68 nM, $p < 0.05$, paired, Student's t-test of treated vs. vehicle, Fig. 2F bottom, G). Furthermore, addition of CT1812 to cultures 1 hour after the addition of Aβ oligomers resulted in a concentration-dependent increase of synaptic number to normal levels (EC50 = 127 nM, Fig. 2G). Examination of synaptic protein expression corroborated these results. Neurogranin is expressed in dendrites and postsynaptic terminals (Fig. 2H), while synaptotagmin-1 is expressed in presynaptic terminals (Fig. 2K) of mature primary hippocampal/cortical neurons in vitro. Aβ oligomer treatment led to a 28% loss of neurons expressing high levels of neurogranin (Fig. 2I) and a 37% loss of synaptotagmin-1 presynaptic terminals (Fig. 2L). Treatment with CT1812 blocked this loss and restored expression of both proteins to control levels (Fig. 2J, M). This suggests that CT1812-mediated displacement of Aβ oligomers from neuronal synapses stops both downstream oligomer-induced synaptic protein downregulation and synapse loss, facilitating synaptic recovery from toxic oligomer insult.

CT1812 displaces Aβ oligomers and facilitates clearance into CSF in vivo and in AD patient brain tissue

To confirm the displacement of Aβ oligomers from cells observed in vitro using an in vivo mouse model of AD, we adapted a novel microimmunoelectrode (MIE) technology previously used to detect rapid kinetic changes in total Aβ concentration in brain interstitial fluid (ISF) [40]

(Supplementary Fig. S3A-E). Using electrodes coated with the oligomer specific antibody A11 [41] placed in the hippocampus, Aβ oligomers were measured in ISF of 12 month old APP_{Swe}/PS1dE9 transgenic mice [42]. A single dose of CT1812 (0.3 μM, or 3.0 μM i.v.) resulted in a rapid and significant increase in Aβ oligomer levels in hippocampal ISF relative to predose baseline (Fig. 3A, vertical dashed line, see Supplementary Fig. S3F). In contrast, no increase was observed in the ISF of vehicle-treated transgenic mice. The rapid elevation of Aβ oligomers after drug administration declined to baseline levels within the timeframe of the recording (120 minutes). In contrast, total Aβ levels (primarily monomer) in the hippocampal ISF were not affected by the administration of CT1812 (Fig. 3B), thus CT1812 selectively reduces Aβ oligomer extracellular concentrations without affecting Aβ monomer levels.

To assess whether CT1812 displacement of Aβ oligomers in AD model systems in vitro and in vivo may also occur in AD patients, we conducted ex vivo binding experiments in 10 μM-thick postmortem neocortical tissue sections obtained from patients with AD (Clinical Dementia Rating (CDR)=3, n=8 patients, Fig. 3C-E). Following incubation of adjacent sections in identical volumes containing increasing concentrations of CT1812 or vehicle, the supernate was removed and the levels of Aβ displaced from the tissue sections quantified by ELISA; the Aβ remaining in the tissue sections was quantified via immunofluorescent microscopy. Analysis of the displaced material by ELISA for total Aβ showed that ascending concentrations of CT1812 increased the amount of Aβ released from the human brain tissue (Fig. 3D): non-denaturing western blots confirmed this material to be Aβ oligomers (Fig. 3C, E, Supplementary Fig. S4). Additionally, CT1812 induced a concentration-dependent decrease in Aβ oligomer immunofluorescence intensity in the 2 μm region containing high concentrations of oligomers surrounding dense, thioflavin-S labeled plaque cores [43,44] (Fig. 3F, G) with similar but not statistically significant changes occurring within the plaque itself (Fig. 3H). These results demonstrate that CT1812 displaces prebound Aβ oligomers from AD patient brain tissue.

Finally, the fate of Aβ oligomers displaced by CT1812 was determined by placing the A11-coated MIE in the lateral ventricle of transgenic APP_{Swe}/PS1dE9 mice to measure Aβ oligomers in the CSF. A significant, dose-dependent rise in Aβ oligomer levels was detected in CSF after drug administration (Fig. 3I) and remained elevated for up to two hours, suggesting that displacement of Aβ oligomers in the brain may lead to increased clearance into the CSF. In contrast, Aβ monomer levels in the CSF were not affected by administration of CT1812 (Fig. 3J), indicating that CT1812 selectively facilitates clearance of oligomers, but not monomers, from the brain into the CSF.

CT1812 improves cognitive performance in transgenic mice

To assess whether this evidence of synapse preservation by CT1812 was associated with functional behavioral improvement, we evaluated changes in cognitive deficits in an aged transgenic mouse model of AD [26,45,46]. Transgenic Thy1 $huAPP^{Swe/Lnd+}$ male mice, aged 3.5 to 4.5 months, or wild-type (WT) littermates were administered vehicle or CT1812 10 mg/kg once daily by oral gavage for 9-10 weeks (n=12 for each group except for the transgenic CT1812-treated group, which was n=13). Treatment of WT mice with CT1812 did not significantly alter motor behavior and did not change cognitive performance compared to that of WT vehicle-treated animals. As expected, significant deficits in transgenic vehicle-treated animals compared to WT vehicle-treated animals were observed in the Activity Chamber test measuring exploration, the Y maze measuring spatial working memory, and the Fear

Conditioning assays measuring aversive associative learning and memory. Significant improvements in spatial learning and memory were observed in animals treated with CT1812 compared to those treated with vehicle in the Water Maze (Fig. 4A), the Y-Maze (Fig. 4B), and in contextual fear conditioning (Fig. 4C). In addition to improving spatial learning and memory, significant improvements were observed in hyperactivity as assessed via the Activity Chamber assay, and cue-dependent learning and memory, as assessed in the Fear Conditioning assay. In wild-type mice, CT1812 had no effect on performance in any of the cognitive tests (Fig. 4A-C).

Previously published studies of eight other sigma-2 receptor antagonists closely related to CT1812 in Thy1 huAPP$^{Swe/Lnd+}$ mice treated daily for 4 weeks-6 months indicated that behavioral improvements were observed as long as brain concentrations of drug were above a theoretical 80% receptor occupancy threshold concentration [26], but that plaque number and Aβ monomer concentration (measured by ELISA) did not change. PK measurements of brain concentrations of CT1812 following treatment of Thy1 huAPP$^{Swe/Lnd+}$ mice with 10 mg/kg p.o. for 9-10 weeks confirmed that this estimated 80% receptor occupancy level was achieved (Fig. 4D, brain concentration 24 hours after last dose = 19.9 ng/mL, 84.4% receptor occupancy, greater than four times the sigma-2 receptor Ki value). Taken together, these studies indicate that threshold brain concentrations of CT1812 effectively improved cognitive deficits found in the huAPP$^{Swe/Lnd+}$ mouse model of AD.

Clinical biomarker evidence of CT1812-mediated synapse protection and disease modification

Following completion of first-in-man clinical studies (NCT02570997 [29]), CT1812 was advanced into clinical trials in AD patients. Mild-to-moderate AD patients with Mini Mental State Exam (MMSE) scores of 18-26 were randomized to receive one of three doses of CT1812 (90 mg, 280 mg, 560 mg) or placebo once daily for 28 days (N=19, 4-5/group) in a double-blind phase 1b/2a clinical trial to determine safety and tolerability (trial COG0102, for full description, see clinicaltrials.gov NCT02907567). The randomized patients, 10 male and 9 female, had a mean age of 70.2 years (SD 9.2) and BMI of 24.75 kg/m^2 (SD 2.73). CSF concentrations at baseline and Day 28 confirmed no presence of CT1812 in the placebo group or at baseline in any dose group. Day 28 mean CSF concentrations of CT1812 rose in a dose-dependent manner (1.15 ng/mL (SD 0.53) in the 90 mg treatment group, 2.84 ng/mL (SD 0.69) in the 280 mg treatment group, and 4.96 (SD 8.49) in the 560 mg treatment group. As expected in a study of limited treatment duration, change in exploratory measures of cognitive function from baseline was similar in CT1812-treated and placebo groups. CSF samples collected from each patient at baseline and at the end of study were used for protein measurements using targeted (i.e., ELISA, western blot, LC-MS/MS) and non-targeted (i.e., unbiased LC-MS/MS proteomics) methods; missing samples and variable sample volumes reduced the number of matched baseline and day 28 patient CSF samples available for subsequent analysis.

Protein gel electrophoresis (western blot) was used to measure Aβ oligomer concentration in CSF samples from each patient taken at Day 0 and 28 and percent change for each patient was calculated. Due to the small number of AD patients in each dosing group, CT1812 dose groups were pooled for comparisons to placebo. After 28 days of treatment, CSF Aβ oligomer concentration (n = 3) in placebo-treated patients trended lower from levels at their own baseline, while levels in CT1812-treated patients (n = 10) increased significantly compared to placebo-treated patients (Fig. 5A and Supplementary Fig. S5). This finding is consistent with preclinical studies indicating that CT1812 displaces and clears toxic Aβ oligomers from the brain into CSF (Fig. 3I) and provides supporting evidence of clinical target engagement. In contrast, Aβ 40 and

42 monomer levels measured with ELISA were not different between Day 0 and Day 28, or between treatment groups in this trial (Supplementary Fig. S5C, D).

The concentrations of several synaptic and axonal proteins are elevated in CSF of AD patients compared to age-matched cognitively normal individuals as a result of CNS synaptic damage due to the disease [47–51]; some markers exhibit greater sensitivity to disease-related changes than do others. We measured concentrations of synaptic and axonal proteins in CSF samples from AD patients in trial COG0102 using ELISA [neurogranin and neurofilament light (NfL)] or targeted LC-MS/MS (synaptotagmin-1, SNAP-25). At 28 days, CSF concentrations of neurogranin and SYT-1 decreased in CT1812-treated AD patients relative to placebo-treated AD patients CSF (Fig. 5B, neurogranin, n = 5 placebo, 11 treated; p=0.050 ANCOVA; Fig 5C, synaptotagmin-1, n = 4 placebo, 9 treated; $F_{1,12} = 8.8$, p = 0.011, linear mixed model), consistent with preclinical evidence of CT1812-mediated facilitation of synaptic recovery from insult with toxic Aβ oligomers. CSF concentrations of NfL and SNAP-25 did not change to a significant degree in CT1812-treated AD patients vs. placebo (Supplementary Fig. S5D, F).

Data from unbiased LC-MS/MS proteomics measurements of CSF were evaluated for effects on synaptic proteins (Fig. 5D). Of the 3160 proteins detected in the CSF of this patient cohort, the abundance of 315 proteins was significantly different between CT1812- and placebo-treated patients (ANOVA followed by Fisher's Least Significant Difference (LSD); $p<0.05$). Pathway analysis using three independent bioinformatics platforms (IPA Canonical Pathway [v51963813], Metacore [v19.4 build 69900], STRING [v11]) indicates that CT1812 significantly ($p<0.05$) impacts synaptic-related pathways including N-methyl-D-aspartate receptor trafficking, glycogen kinase synthase kinase-3β (GSK3β) and WNT signaling, as well as cytoskeletal reorganization. Given the loss of synapses in AD patients along with the preclinical evidence that CT1812 rescues synapse number, we queried which proteins in the synaptic proteome [52] were altered by CT1812 treatment. Twenty five proteins in the synaptic proteome [52] were identified to be differentially expressed (ANOVA followed by Fisher's LSD; $p<0.05$) in CT1812- compared to placebo-treated patient CSF. To understand the functions of these proteins with respect to specific synaptic function in more detail, network analysis was performed. The highest scoring network, Cell Morphology, Cellular Assembly and Organization, Cellular Development, comprised 14 out of 25 of the synaptic proteins, a significantly greater number than expected by random chance (Supplementary Fig. S6A, IPA Score=26; $p<1x10^{-25}$). This indicates that these proteins may play a role in dendritic branching, cytoskeletal remodeling, and neurotransmission (Supplementary Fig. S6B). This provides evidence supporting CT1812's positive effect on synapses in patients with AD.

Out of 520 CSF proteins significantly altered in AD patients vs. age-matched controls ($p<0.05$) in a recent study [53], 334 were detected in the COG0102 CSF proteomics dataset. Of those 334 proteins, a subset of 20 moved in the opposite direction (i.e., reversed AD-related changes) and were also significantly different in CT1812-treated compared to placebo (Fig. 5E). Several of these proteins are involved in key biological pathways known to be disrupted in AD, including cholesterol transport (apolipoprotein A2; APOA2), oxidative stress (ceruloplasmin; CP), complement (complement C1r subcomponent-like protein; C1RL), and synaptic transmission (14-3-3 protein beta/alpha; YWHAZ). This provides supporting evidence for a broad improvement of disease-related signaling by CT1812 in patients with AD.

One of the hallmarks of AD is hyperphosphorylated tau protein, which comprises neurofibrillary tangles (NFTs) [54–58]. We evaluated AD patient CSF for concentrations of unphosphorylated

and phosphorylated tau protein fragments taken at baseline and after 28 days of CT1812 or placebo treatment via LC-MS/MS (Fig. 5F); phosphorylated peptide fragments representing 33 distinct phosphorylation sites on tau were detected. The abundance of 6 phosphorylation sites decreased by 30% or more (Fig. 5F) [59,60] after treatment with CT1812 compared to placebo while one site increased more than 30% (the threshold for noise distribution [61]), but the concentration of unphosphorylated tau did not change. In agreement with these results, ELISA measurements of the change from baseline of phospho tau (P-tau) (181) and total tau (T-tau) was similar in CT1812-treated and placebo groups (Supplementary Fig. S5E, F). Additionally, LC-MS/MS measurements of concentrations of kinases that phosphorylate tau, such as GSK3β trended lower by 25% in CT1812-treated patients (not significantly different from placebo-treated patients, p=0.098). These results suggest that CT1812 may act upstream of tau kinases to reduce their concentration and resulting activity, while having no impact on tau expression or regulation. In order to identify phosphorylation sites within tau that might covary in abundance in response to CT1812 treatment, correlation analyses were performed and a heatmap was generated. The abundance of 21 pairs of P-tau sites was found to be significantly correlated with one another (Supplementary Fig. S7), supporting the hypothesis that CT1812 may act upstream of tau kinases/phosphatase to impact tau phosphorylation at specific amino acid sites. Taken together, these clinical biomarker data support a potential therapeutic impact of CT1812 in patients with AD.

Discussion

CT1812 displaces Aβ oligomers in several preclinical models of AD

The Aβ oligomer hypothesis remains a compelling rationale for AD drug development programs [2]. Supporting evidence for this comes from the genetic determinants of autosomal dominant AD and AD complicating Down syndrome [62], the protective effect of the Icelandic mutation of the amyloid precursor protein [5,6] animal data indicating the toxic effects of Aβ oligomer species on synaptic function [8,63] and its reversibility [27], and the observation that Aβ accumulation alone in cognitively and clinically normal individuals predicts symptomatic AD with high likelihood [64]. Drug development programs targeting Aβ include active and passive Aβ immunotherapeutics [7] and secretase inhibitors that decrease Aβ peptide generation [65], but none effectively or selectively target Aβ oligomers.

The current study demonstrates that CT1812 displaces Aβ oligomers from neurons with 3 independent approaches: in vitro cell culture, in vivo rodent studies (including two different mouse models of AD), and ex vivo human brain CSF and tissue. In cultured rat brain cells in vitro, CT1812 shifted the binding of exogenously applied, synthetic Aβ oligomers to lower affinity whether added before or after oligomers. Importantly, CT1812-mediated reduction of oligomer affinity phenocopies or mimics the effect of the Alzheimer's protective Icelandic mutation on oligomer affinity [66], and is the only drug candidate currently in development reported to do so. This is significant because drug candidates with the same mechanism as protective variants are expected to have a higher success rate in the clinic [67]. CT1812 treatment for 1 hour did not decrease the intensity of pre-bound Aβ oligomers as completely as it did when added to cultures prior to the oligomers. It is possible that longer treatment with CT1812 can achieve a greater level of displacement. However, incubation with Aβ oligomers for longer times results in internalization of a portion of the Aβ oligomer labeling [26], complicating quantification of the compound treatment. Nonetheless, our results demonstrate that CT1812 both displaces already-bound Aβ oligomers and prevents the binding of Aβ oligomers to

neuronal synaptic receptors; displaced oligomers will not re-bind as long as CT1812 remains present. Thus, CT1812 will likely continue to exert its effect as concentrations of oligomers rise throughout the course of AD. In separate biochemical assays using an oligomer-specific ELISA, CT1812 does not interact directly with oligomers and did not disrupt preformed oligomers or block oligomer formation (Supplemental Fig. S2). In postmortem human AD brain tissue sections, CT1812 caused a concentration-dependent increase in Aβ displaced from the tissue as measured by Aβ ELISA, as well as a concentration-dependent increase in several oligomeric species of Aβ as detected by western blot analysis of the material displaced from the tissue [68]. This was accompanied by a decrease in Aβ within the tissue section in the 2 micron oligomer-enriched halo surrounding plaques. While we cannot rule out compound-mediated displacement of oligomers from extrasynaptic sites that are below the level of detection of our imaging methods, oligomers that are dose-dependently displaced by CT1812 are highly likely to originate from synaptic receptor sites; because oligomers are water-soluble, oligomers in the interstitial fluid in these frozen tissue sections should freely diffuse in any aqueous media and be detectable in the vehicle treated condition as well (Fig 3C-E). The transgenic mouse MIE measurements provide additional insight on the selectivity of CT1812's effect on oligomers: a single dose of CT1812 rapidly increased concentrations of Aβ oligomer, but not Aβ monomer in brain. Together, these results demonstrate that CT1812 is a dose-dependent, negative allosteric modulator of Aβ oligomer binding.

Unexpectedly, these same measurements provided evidence suggesting that CT1812 directly or indirectly facilitates clearance of Aβ oligomer, but not monomer, out of the brain and into the CSF; it rapidly increases ISF and CSF concentrations of oligomers in a dose-dependent manner, but not monomers. The difference in kinetic rate of increase in Aβ oligomer concentration between the hippocampus and lateral ventricle may result from different electrode sampling volumes due to diffusion constraints within brain tissue compared to CSF. The basis for this selective clearance of Aβ oligomers but not monomers is currently unclear. While mechanisms of Aβ monomer clearance from the brain into CSF have been studied extensively (reviewed in [40]), oligomer clearance mechanisms are currently unknown. One possible mechanism is suggested by recent studies demonstrating direct interactions of sigma-2 receptor complex component proteins PGRMC1 and TMEM97 with LDL receptor, required for ligand-bound LDL receptor internalization [31], and sigma-2 receptor-mediated cellular uptake of Aβ via interactions with apolipoproteins and the LDL receptor [31,69]. Previously tested closely related sigma-2 receptor antagonists do not impact monomer or fibril levels in Thy1 huAPP$^{Swe/Lnd+}$ transgenic mice following chronic short term administration [26]. To more fully explore the role of these proteins in AD, future studies (including studies in AD mouse models cross-bred with conditional tissue-specific knockouts of each protein to avoid lethality) are required.

We hypothesize that displacement of toxic Aβ oligomers from synaptic receptor sites and clearance of oligomer into the CSF underlies the improvement of cognitive performance in transgenic AD mice seen with chronic CT1812 administration. As with other closely related sigma-2 receptor antagonists [26], CT1812 improves transgenic mouse behavior at brain concentrations corresponding to an estimated 80% receptor occupancy; typical for an antagonist mechanism of action, threshold concentrations of drug are required to block effects. While CT1812's in vitro assay EC50 values range from high nanomolar to low micromolar concentrations, behavioral improvement is observed at brain concentrations closer to CT1812's Ki at sigma-2 receptors (8.5 nM). The basis for this difference is unclear but may be due to the short duration and high concentrations of synthetic Aβ oligomers used in the in vitro assays.

Once displaced from synaptic receptors, the oligomers are no longer able to harm synapses and are subject to elimination through yet to be defined clearance pathways.

Preliminary biomarker evidence for CT1812 target engagement and disease-modification in patients with AD

Protein measurements of CSF samples from the 28-day clinical trial COG0102 provide preliminary evidence of target engagement and potential impact on disease in mild-to-moderate AD patients consistent with preclinical data. CSF concentrations of Aβ oligomers increase in CT1812-treated patients vs. placebo similar to preclinical studies, indicating that CT1812 displaces and clears toxic Aβ oligomer from the brain into CSF. CSF concentrations of the postsynaptic dendritic protein neurogranin, typically significantly elevated in AD patients [51,70–72] are reduced by CT1812 treatment, compared with changes in placebo patients. Additionally, several synaptic proteins are significantly different in CT1812- vs. placebo-treated patients; bioinformatics analysis of these changes support preclinical evidence of a positive impact of CT1812 on synaptic pathways.

Analysis of CSF concentrations of phosphorylated tau fragments in AD patients revealed that treatment with CT1812 induced a broad reduction in tau phosphorylation at multiple amino acid sites without affecting unphosphorylated tau concentration. Many of the residues altered by CT1812 treatment have been previously implicated in AD-related changes [73–78]. Data correlating phosphorylation at any given amino acid of tau with disease progression in patients (as well as how closely mouse disease models reflect such changes) are still emerging.

Preclinical evidence demonstrates that Aβ oligomer binding results in upregulation of tau kinase activity [2] leading to tau phosphorylation at multiple sites. The observed reduction in GSK3β as well as tau phosphorylation in CT1812-treated patients provides the first clinical biomarker evidence supporting the Aβ oligomer hypothesis of AD and further support of CT1812's disease-modifying mechanism of action.

We hypothesize that changes in CSF concentration of a subset of proteins with CT1812 treatment reflect target engagement in the brain. Further clinical studies with longer treatment duration are underway; treatment-related impact on biomarkers in these independent clinical cohorts will provide additional insight on CT1812 target engagement and AD pathobiology as well as insight into how covariates like sex, age, and ApoE status impact response to drug. The effects of these changes in CSF protein concentrations on cognition and health is unknown and the relative benefit of these effects compared to the risks of the drug are being determined in ongoing and future placebo-controlled clinical trials.

CT1812 for the treatment of AD

The hypothesized disease-modifying mechanism of action of CT1812 is illustrated in Figure 6. In the normal brain (Fig. 6A), the sigma-2 receptor complex regulates the plasma membrane surface expression of putative Aβ oligomer receptor complex component proteins LilRB2, Nogo and cellular prion protein as well as several other receptors [79] (Fig. 6B). In AD, Aβ oligomers bind to their receptor, altering its function and/or protein interactions, and resulting in a compensatory upregulation of the sigma-2 receptor complex (Fig. 6C) [80,81]. The binding of Aβ oligomers then leads to synaptic damage and release of presynaptic and postsynaptic proteins such as neurogranin and synaptotagmin-1 into the ISF and CSF (Fig. 6D). CT1812 binds to and allosterically modulates the sigma-2 receptor (Fig. 6E), causing destabilization of the

neighboring Aβ oligomer receptor binding sites with resultant displacement of Aβ oligomers from synaptic receptors (i.e., increase in the "off rate") without affecting normal synaptic protein function. CT1812 is thus a negative allosteric modulator of Aβ oligomer binding to synaptic receptors. As a result of the removal of toxic oligomers, synapse number and memory are restored to normal (Fig. 6F). CT1812 selectively displaces Aβ oligomers shortly after entering the brain and prevents them from rebinding as long as brain drug levels remain above an estimated 80% receptor occupancy [26]. Chronic administration provides sustained protection from the synaptotoxic oligomer assault, facilitating synaptic recovery.

The current studies suggest that CT1812 effectively and selectively targets Aβ oligomers by a novel mechanism of action not previously demonstrated for any other therapeutics currently in development. CT1812 is both the first selective sigma-2 receptor antagonist to be used in clinical trials, and the first therapeutic demonstrated to displace toxic Aβ oligomers from synaptic receptor sites and selectively facilitate their clearance into the CSF. Displacement of oligomers lowers their binding affinity (K_D) to synaptic receptors significantly, thus CT1812 is the only therapeutic currently in development that mimics the effect of the protective Icelandic A673T mutation [6]. This mechanism is significant, as therapeutics that recapitulate the effects of protective mutations have a track record of clinical success [67].

Currently approved AD medications do not stop the disease course, but simply treat symptoms for a limited time. These preclinical results of CT1812 in rodent models of AD demonstrate that CT1812 blocks Aβ oligomer binding to neurons, reduces synapse loss, restores synaptic protein expression, facilitates oligomer clearance into the CSF, and restores cognitive function. The ability of CT1812 to improve cognitive performance in transgenic mice while not affecting the performance of wild-type mice supports a specific effect of CT1812 on the pathological pathway of AD: this disease-selective mechanism may provide an advantage over other therapeutic approaches that impact brain function more widely.

Preliminary evidence from the phase1b/2a clinical trial reported here supports these findings. This study was limited by small patient numbers and short duration of treatment in the COG0102 trial. Larger studies with additional dose levels will be required to establish dose-response relationships with biomarker changes, and distingish both acute and long-term disease modifying effects of Ct1812 treatment. While not all proteins and signaling pathways known to be dysregulated in AD were affected by treatment with CT1812, several pathways were significantly impacted (including cholesterol transport, oxidative stress, complement, and synaptic transmission; Fig. 5E). Together, these results provide encouraging evidence of the impact of CT1812 on multiple aspects of disease in AD patients and support further development of this drug candidate so that the relative benefit and risks of CT1812 can be more thoroughly evaluated.

CT1812 is an investigational therapeutic that has not been reviewed or approved for any use by FDA. CT1812 is currently being studied in four randomized, double-blind, placebo-controlled phase 2 studies (6 months – 1 year in treatment duration) in patients with mild to moderate AD: SNAP (NCT03522129), SPARC (NCT03493282), SHINE (NCT03507790), and SEQUEL. An additional 18 month study in 540 early AD patients (MMSE 20-30) is being planned in collaboration with the ACTC clinical trial network. The safety and tolerability of CT1812 will continue to be explored in all clinical trials.

Materials and Methods

Radioligand binding

Radioligand competition assays to determine affinity for sigma-2 and sigma-1 receptors were performed at Eurofins Cerep SA (Le Bois L'évêque, France) in membranes from Jurkat cells (immortalized human T cells). Assays for sigma-2 receptors used 25 nM [^{3}H]1,3-di(2-tolyl) guanidine in the presence of 1 μM (+)-pentazocine while assays for sigma-1 receptors used 15 nM [^{3}H](+)-pentazocine. Non-specific binding in both assays was defined in the presence of 10 μM haloperidol [82]. Estimated percent receptor occupancy for in vivo behavioral studies (see below) was calculated according to the formula 100*(concentration/Ki)/[(concentration/Ki) + 1)], where Ki is determined by radioligand competition binding (CT1812 = 8.5 nM) [26].

Neuronal cultures

Mixed neuronal and glia cultures were made from embryonic day 18 (E18) Sprague Dawley rat brains and grown in poly-D Lysine coated plates for 21 days, as previously described [26,28]. All procedures were approved by the Institutional Animal Care and Use and Committee at Cognition Therapeutics and were in compliance with the Office of Laboratory Animals Welfare and the Guide for the Care and Use of Laboratory Animals, Eighth Edition. Embryos from a single rat were pooled to produce a unique dissociated neuronal culture. All analyses described below were performed on at least three unique cultures. Healthy cultures typically contain 20%-35% MAP2-positive neurons. CT1812 was tested in quadruplicate wells for each concentration in at least three replicate experiments with data from all experiments pooled for analysis with means +/- standard deviation (SD) or standard error of the mean (SEM) as noted.

Aβ Oligomer preparation

Synthetic human Aβ 1-42 peptide was prepared as previously described [26,28]. Briefly, peptide was treated according to published methods to remove any structural assemblies [83,84]. An Aβ monomer film was prepared, dissolved, diluted to 100 μM, and incubated at 4 ºC to form oligomers. The resulting preparations were centrifuged to remove any insoluble fibrils, and the supernate added to cultures. All studies using synthetic oligomers were performed with this preparation unless otherwise specified. All lots of Aβ 1-42 are put through a strict quality control processes, described previously [26,28], before use in experiments. As previously reported, oligomers produced via this method typically range from 25-275 kDa when measured via non-denatured western blots (Figure 2, [26]).

Human AD patient (Braak V/VI) and age-matched control hippocampal brain specimens, less than 24 hours post-mortem, were obtained from the Brown Brain Bank following previously described procedures [26,28]. Tissue was prepared as previously described [26,28]. Briefly, the brain tissue was homogenized and centrifuged, supernate were immuno-depleted and concentrated to obtain the10-100 kDa size-fractionated oligomers, which were then captured on 6E10-conjugated agarose columns (Pierce). The released material was desalted and stored at -80 ºC. Use of postmortem brain specimens met the exemption criteria for DHHS regulations, as previously explained [26,28].

In vitro trafficking assay

Vesicular trafficking was measured using an adaptation of a method as previously described [26,85]. Neurons were treated with compounds and/or Aβ oligomer preparations (0.086% DMSO in culture media) and incubated for 1 to 24 hours at 37ºC in 5% CO2. For prevention studies, CT1812 was added at indicated concentrations 1 hour prior to addition of Aβ oligomers. In

treatment studies, Aβ oligomers were added 1 hour prior to addition of CT1812. Tetrazolium salts (3-(4,5-dimethylthiazol-2yl)-2,5diphenyl tetrazolium bromide, Roche Molecular Biochemicals) were added at a final concentration of 0.75 mM and incubated at 37ºC for 60-90 min. Vesicular formazan remaining in cells was quantified by absorbance spectrometry (590 nm with 690 nm subtracted) following extraction with 1.6% Tween-20. All compounds were tested in quadruplicate wells for each concentration in at least 8 replicate experiments with data from all experiments pooled for analysis with means ± SEM.

In vitro Aβ binding assay

Assessment of Aβ oligomer binding was performed as previously described [26,28]. Briefly, cultures were either (for prevention studies) treated with CT1812 for 30 minutes, followed by synthetic Aβ 1-42 oligomer preparation for 60 min, or (for displacement studies) treated with oligomers 30 min prior to the addition of CT1812. Cells were then fixed and labeled for immunofluorescent microscopy as previously described [26]. All data for Aβ binding presented represents total fluorescent intensity of Aβ label in neurite spots per neuron in relative fluorescent units (RFU). Replications and statistical procedures for the quantification of Aβ immunofluorescent intensity were previously described [26].

In vitro synapse counting assay

Synapse number was quantified using quantitative immunofluorescent microscopy of drebrin-labeled puncta (Millipore AB-10140) along MAP2-positive neurites (Millipore AB5543) as previously described [26]. Additional immunofluorescent labeling was performed on neuronal cultures for SYT-1 (Synaptic Systems #105 103) and for neurogranin (Abcam ab23570).

Human tissue ex vivo Aβ displacement

Displacement of Aβ from human tissue was assessed as previously described [28]. Briefly, brains from human AD patients were obtained through the Massachusetts Alzheimer's Disease Research Center and Massachusetts General Hospital (MGH) Neuropathology Department. Experiments using human brain were reviewed and approved by the Academic and Clinical Central Office for Research and Development medical research ethics committee, a joint office of the University of Edinburgh and NHS Lothian (approval 15-HV-016). Parahippocampal gyrus sections (one section per specimen per condition) were incubated with 0.1, 1.0, 10, or 15 μM CT1812 in PBS, or vehicle for 60 min as previously described [26] and then labeled with an antibody specific to Aβ (AW-7, gift from Dominic Walsh [86]). Dense core amyloid plaques and neurofibrillary tangles were labeled with 0.05% Thioflavin-S (Sigma Aldrich) in 50% ethanol for 8 min before treatment with 80% ethanol for 30 s. Images were analyzed in ImageJ [87] using a custom macro (described in Fig. S4 in Izzo, et al. 2014b [28]). A total of 105 to 279 plaques were analyzed for each treatment from eight different donors and average intensities for each specimen were calculated. The median intensity value was calculated for each specimen and subjected to multivariate correlation analysis as previously described [28]. Determination of total Aβ concentration eluted from human donor brain tissue was performed using a high sensitivity, human Beta Amyloid (1-42) ELISA Kit (Wako, cat # 296-64401) which uses [BAN50/BC05 (Fab')].

Western blot analysis of Aβ oligomers

Non-denaturing western blot conditions were employed to avoid the generation of Aβ assembly and disassembly artifacts, as previously described [26]. Briefly, baseline and end of study CSF

samples from AD patients participating in clinical trial COG0102 were collected in polypropylene tubes in 500 µL and frozen at -80ºC until analysis. Upon receipt, the samples were thawed and quickly aliquoted into polypropylene tubes coated with isotonic human serum albumin and refrozen until analysis by native western gels. Because the effects of blood on Aβ oligomer formation in CSF is unknown, an aliquot of each patient sample was pre-analyzed on a western blot using luminol and horseradish peroxide to test for the presence of heme. Final western gel analysis was performed on samples excluding those containing hemolyzed blood. Samples were run on Tris-HCl nondenaturing gels, transferred to nitrocellulose and probed with 82E1 mouse monoclonal Aβ antibody (IBL America, Minneapolis, MN) and visualized by chemiluminescence after detection using a goat anti mouse IgG-horseradish peroxidase secondary antibody (Millipore, Burlington, MA). All reagents were filtered through 0.1 micron filters to eliminate background debris. Band intensities on the gels were quantified using an Alpha Innotech image system and Alpha View software (ProteinSimple, San Jose, CA). Each patient's sample at day 28 was normalized as a percent of that patient's own baseline value.

Measurement of Aβ using microimmunoelectrodes

APP/PS1+/− hemizygous mice [42] were bred to wildtype C3H/B6 mice (The Jackson Laboratory) and the APP/PS1+/− offspring were used for experiments at 12 months of age. Male and female littermate mice were distributed between experimental groups.

MIEs, which can measure Aβ every 60 seconds for up to three hours, were prepared similar to previously described methods [40]. Carbon fiber microelectrodes were used as the platform sensor due to their high signal to noise ratio, biological compatibility, and miniature size [88], and ability to sensitively detect tyrosine oxidation (66). Electrodes were coated with antibodies specific for Aβ monomer (HJ2)[40] or for oligomers (A11)[41] and inserted into hippocampus to measure brain ISF Aβ levels or into lateral ventricles to measure CSF Aβ levels.

Electrodes were pre-calibrated in vitro (see supplementary methods). In addition to the MIE, a stainless-steel bone screw used as a counter electrode and an Ag/AgCl reference electrode (InVivo Metrics, CA USA) were implanted into the brains of 12-month old APP/PS1+/- transgenic mice. All electrodes were stereotaxically implanted under isofluorane anesthesia. Mice were placed on a heating pad to maintain body temperature and repetitive SWV scans were run every 60 s for up to 180 min using a CH Instruments 830D Electrochemical Analyzer with PicoAmp booster. The stereotax was enclosed in a faraday cage to reduce electrical noise. CT1812 or vehicle were administered i.v. via tail vein injection at the concentrations noted. All procedures were approved by the Institutional Animal Care and Use and Committee at Washington University, St Louis, and were in compliance with the Office of Laboratory Animals Welfare and the Guide for the Care and Use of Laboratory Animals, Eighth Edition.

More detail can be found in the supplementary methods section.

Behavioral Studies

All procedures were approved by the Institutional Animal Care and Use and Committee at Stanford University and were in compliance with the Office of Laboratory Animal Welfare and the Guide for the Care and Use of Laboratory Animals, Eighth Edition. Testing of male transgenic Thy1 huAPP$^{Swe/Lnd+}$ mice in the Morris water maze, Y-Maze, or fear conditioning tasks was done according to published methods [45,46]. Studies were designed with four arms: wild-type, vehicle treated (n = 12); wild type, CT1812 treated (n = 12); transgenic, vehicle

treated (n = 12); transgenic, CT1812 treated (n = 13). All procedures were approved by the Institutional Animal Care and Use and Committee at Stanford University and were in compliance with the Office of Laboratory Animals Welfare and the Guide for the Care and Use of Laboratory Animals, Eighth Edition.

To measure brain concentration of drugs, brains were homogenized in 1 ml PBS per gram of brain tissue using a handheld homogenizer. Brain homogenate was then extracted with three volumes of ice cold methanol on ice for 15 minutes and centrifuged for 15 min. The supernates were analyzed by LC/MS/MS. Samples were compared to a calibration curve prepared in a similar manner by spiking blank control homogenate with standards prepared in DMSO and then extracted as above.

Clinical trial of CT1812 in mild-to-moderate AD patients

The clinical trial was performed at six sites in Australia and administered by Neuroscience Trials Australia. The study protocol was approved by the Human Research Ethics Committee at the Alfred Hospital, Melbourne, Australia, and was conducted in accordance with the Declaration of Helsinki and Good Clinical Practice guidelines. All subjects provided written informed consent before participating. Mild to moderate (MMSE 18-26) AD patients (N=19) were randomized to one of three doses of CT1812 (90, 280 or 560 mg Q.D.) or placebo given orally once daily for 28 days (4 weeks) to determine safety and tolerability (COG0102, for full listing of inclusion and exclusion criteria see ClinicalTrials.gov NCT02907567). Exploratory outcomes included CSF protein expression measured at baseline (Day 0) and end of treatment (Day 28). Missing samples (declined or failed spinal taps) and variable CSF sample volumes reduced the number of matched baseline and day 28 patient CSF samples available for subsequent analysis.

ELISA measurement of CSF synaptic proteins

CSF levels of Aβ40, Aβ42, T-tau and P-tau were measured using the INNOTEST enzyme-linked immunosorbent assays (ELISA) (Fujirebio, Ghent, Belgium), following the recommendations by the manufacturer. Neurofilament light was measured using an ELISA from Uhman Diagnostics (Umea, Sweden). These analyses were conducted by board-certified laboratory technicians according to Swedish Board for Accreditation and Conformity Assessment (SWEDAC)-approved protocols. Neurogranin CSF concentrations were measured using an in-house ELISA method based on the Ng2 and Ng22 antibodies, as described previously in detail [89]. Concentrations of SNAP-25 in CSF were measured using immunoprecipitation combined with mass spectrometry (IP-MS) as described previously [90].

LC-MS/MS measurement of CSF synaptic proteins and phosphorylated tau fragments

Synaptotagmin-1 measurements were obtained as part of unbiased LC-MS/MS proteomics analysis of AD patient CSF samples at Caprion Biosciences using published methods [91]. Additional unbiased proteomics analyses including an enrichment for phospho-proteome were performed on CSF samples at Proteome Sciences using the protocols as previously published [61,92] with minor modifications. For statistical analysis of unbiased LC-MS-MS proteomics, a linear mixed model was used. Detailed methods can be found in the supplementary methods section.

References

[1] Cummings J, Lee G, Ritter A, Sabbagh M, Zhong K. Alzheimer's disease drug development pipeline: 2019. Alzheimer's Dement Transl Res Clin Interv 2019;5:272–93.

https://doi.org/10.1016/j.trci.2019.05.008.

[2] Selkoe DJ, Hardy J. The amyloid hypothesis of Alzheimer's disease at 25 years. EMBO Mol Med 2016;8:595–608. https://doi.org/10.15252/emmm.201606210.

[3] Hardy J. The Discovery of Alzheimer causing Mutations in the APP Gene and the Formulation of the "Amyloid Cascade Hypothesis". FEBS J 2017;38:42–9. https://doi.org/10.1111/febs.14004.

[4] Walsh DM, Selkoe DJ. Amyloid β-protein and beyond: the path forward in Alzheimer's disease. Curr Opin Neurobiol 2020;61:116–24. https://doi.org/10.1016/j.conb.2020.02.003.

[5] Jonsson T, Atwal JK, Steinberg S, Snaedal J, Jonsson P V, Bjornsson S, et al. A mutation in APP protects against Alzheimer's disease and age-related cognitive decline. Nature 2012;488:96–9. https://doi.org/10.1038/nature11283.

[6] Limegrover CS, LeVine H, Izzo NJ, Yurko R, Mozzoni K, Rehak C, et al. Alzheimer's protection effect of A673T mutation may be driven by lower Aβ oligomer binding affinity. J Neurochem 2020:jnc.15212. https://doi.org/10.1111/jnc.15212.

[7] van Dyck CH. Anti-Amyloid-β Monoclonal Antibodies for Alzheimer's Disease: Pitfalls and Promise. Biol Psychiatry 2018;83:311–9. https://doi.org/10.1016/j.biopsych.2017.08.010.

[8] Viola KL, Klein WL. Amyloid beta oligomers in Alzheimer's disease pathogenesis, treatment, and diagnosis. Acta Neuropathol 2015;129:183–206. https://doi.org/10.1007/s00401-015-1386-3.

[9] Park J, Strittmatter S. Nogo Receptor Interacts with Brain APP and Aβ to Reduce Pathologic Changes in Alzheimers Transgenic Mice. Curr Alzheimer Res 2007;4:568–70. https://doi.org/10.2174/156720507783018235.

[10] Kim T, Vidal GS, Djurisic M, William CM, Birnbaum ME, Garcia KC, et al. Human LilrB2 is a β-amyloid receptor and its murine homolog PirB regulates synaptic plasticity in an Alzheimer's model. Science 2013;341:1399–404. https://doi.org/10.1126/science.1242077.

[11] Smith LM, Kostylev MA, Lee S, Strittmatter SM. Systematic and standardized comparison of reported Amyloid-β receptors for sufficiency, affinity, and Alzheimer's disease relevance. J Biol Chem 2019:jbc.RA118.006252. https://doi.org/10.1074/jbc.RA118.006252.

[12] Shrestha BR, Vitolo O V, Joshi P, Lordkipanidze T, Shelanski M, Dunaevsky A. Amyloid beta peptide adversely affects spine number and motility in hippocampal neurons. Mol Cell Neurosci 2006;33:274–82. https://doi.org/10.1016/j.mcn.2006.07.011.

[13] Lacor PN, Buniel MC, Furlow PW, Clemente AS, Velasco PT, Wood M, et al. Abeta oligomer-induced aberrations in synapse composition, shape, and density provide a molecular basis for loss of connectivity in Alzheimer's disease. J Neurosci 2007;27:796–807. https://doi.org/10.1523/JNEUROSCI.3501-06.2007.

[14] Shankar GM, Li S, Mehta TH, Garcia-Munoz A, Shepardson NE, Smith I, et al. Amyloid-beta protein dimers isolated directly from Alzheimer's brains impair synaptic plasticity

and memory. Nat Med 2008;14:837–42. https://doi.org/10.1038/nm1782.

[15] Calabrese B, Shaked GM, Tabarean I V, Braga J, Koo EH, Halpain S. Rapid, concurrent alterations in pre- and postsynaptic structure induced by naturally-secreted amyloid-beta protein. Mol Cell Neurosci 2007;35:183–93. https://doi.org/10.1016/j.mcn.2007.02.006.

[16] Wang D, Govindaiah G, Liu R, De Arcangelis V, Cox CL, Xiang YK. Binding of amyloid beta peptide to beta2 adrenergic receptor induces PKA-dependent AMPA receptor hyperactivity. FASEB J 2010;24:3511–21. https://doi.org/10.1096/fj.10-156661.

[17] Lambert MP, Barlow a K, Chromy B a, Edwards C, Freed R, Liosatos M, et al. Diffusible, nonfibrillar ligands derived from Abeta1-42 are potent central nervous system neurotoxins. Proc Natl Acad Sci U S A 1998;95:6448–53.

[18] Li S, Hong S, Shepardson NE, Walsh DM, Shankar GM, Selkoe D. Soluble Oligomers of Amyloid β Protein Facilitate Hippocampal Long-Term Depression by Disrupting Neuronal Glutamate Uptake. Neuron 2009;62:788–801. https://doi.org/10.1016/j.neuron.2009.05.012.

[19] Wang Q, Walsh D, Rowan MJ, Selkoe DJ, Anwyl R. Block of Long-Term Potentiation by Naturally Secreted and Synthetic Amyloid -Peptide in Hippocampal Slices Is Mediated via Activation of the Kinases c-Jun N-Terminal Kinase, Cyclin-Dependent Kinase 5, and p38 Mitogen-Activated Protein Kinase as well as Me. J Neurosci 2004;24:3370–8. https://doi.org/10.1523/JNEUROSCI.1633-03.2004.

[20] Walsh DM, Klyubin I, Fadeeva J V., Cullen WK, Anwyl R, Wolfe MS, et al. Naturally secreted oligomers of amyloid β protein potently inhibit hippocampal long-term potentiation in vivo. Nature 2002;416:535–9. https://doi.org/10.1038/416535a.

[21] Walsh DM, Townsend M, Podlisny MB, Shankar GM, Fadeeva J V, El Agnaf O, et al. Certain inhibitors of synthetic amyloid beta-peptide (Abeta) fibrillogenesis block oligomerization of natural Abeta and thereby rescue long-term potentiation. J Neurosci 2005;25:2455–62. https://doi.org/10.1523/JNEUROSCI.4391-04.2005.

[22] Klyubin I, Walsh DM, Lemere CA, Cullen WK, Shankar GM, Betts V, et al. Amyloid β protein immunotherapy neutralizes Aβ oligomers that disrupt synaptic plasticity in vivo. Nat Med 2005;11:556–61. https://doi.org/10.1038/nm1234.

[23] Klyubin I, Betts V, Welzel AT, Blennow K, Zetterberg H, Wallin A, et al. Amyloid beta protein dimer-containing human CSF disrupts synaptic plasticity: prevention by systemic passive immunization. J Neurosci 2008;28:4231–7. https://doi.org/10.1523/JNEUROSCI.5161-07.2008.

[24] Puzzo D, Vitolo O, Trinchese F, Jacob JP, Palmeri A, Arancio O. Amyloid-beta peptide inhibits activation of the nitric oxide/cGMP/cAMP-responsive element-binding protein pathway during hippocampal synaptic plasticity. J Neurosci 2005;25:6887–97. https://doi.org/10.1523/JNEUROSCI.5291-04.2005.

[25] Puzzo D, Privitera L, Leznik E, Fà M, Staniszewski A, Palmeri A, et al. Picomolar amyloid-beta positively modulates synaptic plasticity and memory in hippocampus. J Neurosci 2008;28:14537–45. https://doi.org/10.1523/JNEUROSCI.2692-08.2008.

[26] Izzo NJ, Staniszewski A, To L, Fa M, Teich AF, Saeed F, et al. Alzheimer's therapeutics

targeting amyloid beta 1-42 oligomers I: Abeta 42 oligomer binding to specific neuronal receptors is displaced by drug candidates that improve cognitive deficits. PLoS One 2014;9:e111898. https://doi.org/10.1371/journal.pone.0111898.

[27] Cleary JP, Walsh DM, Hofmeister JJ, Shankar GM, Kuskowski M a, Selkoe DJ, et al. Natural oligomers of the amyloid-beta protein specifically disrupt cognitive function. Nat Neurosci 2005;8:79–84. https://doi.org/10.1038/nn1372.

[28] Izzo NNJ, Xu J, Zeng C, Kirk MJ, Mozzoni K, Silky C, et al. Alzheimer's therapeutics targeting amyloid beta 1-42 oligomers II: Sigma-2/PGRMC1 receptors mediate Abeta 42 oligomer binding and synaptotoxicity. PLoS One 2014;9:e111899. https://doi.org/10.1371/journal.pone.0111899.

[29] Grundman M, Morgan R, Lickliter JD, Schneider LS, DeKosky S, Izzo NJ, et al. A phase 1 clinical trial of the sigma-2 receptor complex allosteric antagonist CT1812, a novel therapeutic candidate for Alzheimer's disease. Alzheimer's Dement (New York, N Y) 2019;5:20–6. https://doi.org/10.1016/j.trci.2018.11.001.

[30] Oyer HM, Sanders CM, Kim FJ. Small-Molecule Modulators of Sigma1 and Sigma2/TMEM97 in the Context of Cancer: Foundational Concepts and Emerging Themes. Front Pharmacol 2019;10:1141. https://doi.org/10.3389/fphar.2019.01141.

[31] Riad A, Zeng C, Weng C-CC, Winters H, Xu K, Makvandi M, et al. Sigma-2 Receptor/TMEM97 and PGRMC-1 Increase the Rate of Internalization of LDL by LDL Receptor through the Formation of a Ternary Complex. Sci Rep 2018;8:16845. https://doi.org/10.1038/s41598-018-35430-3.

[32] Ahmed ISA, Chamberlain C, Craven RJ. S2R(Pgrmc1): the cytochrome-related sigma-2 receptor that regulates lipid and drug metabolism and hormone signaling. Expert Opin Drug Metab Toxicol 2012;8:361–70. https://doi.org/10.1517/17425255.2012.658367.

[33] Cahill MA. Progesterone receptor membrane component 1: an integrative review. J Steroid Biochem Mol Biol 2007;105:16–36. https://doi.org/10.1016/j.jsbmb.2007.02.002.

[34] Cahill MA, Jazayeri JA, Catalano SM, Toyokuni S, Kovacevic Z, Richardson DR. The emerging role of progesterone receptor membrane component 1 (PGRMC1) in cancer biology. Biochim Biophys Acta 2016;1866:339–49. https://doi.org/10.1016/j.bbcan.2016.07.004.

[35] Nguyen T, Su C, Singh M. Let-7i inhibition enhances progesterone-induced functional recovery in a mouse model of ischemia. Proc Natl Acad Sci U S A 2018;115:E9668–77. https://doi.org/10.1073/pnas.1803384115.

[36] Su C, Cunningham RL, Rybalchenko N, Singh M. Progesterone increases the release of brain-derived neurotrophic factor from glia via progesterone receptor membrane component 1 (Pgrmc1)-dependent ERK5 signaling. Endocrinology 2012;153:4389–400. https://doi.org/10.1210/en.2011-2177.

[37] Izzo NJ, Colom-Cadena M, Riad AA, Xu J, Singh M, Abate C, et al. Proceedings from the Fourth International Symposium on sigma-2 Receptors: Role in Health and Disease. ENeuro 2020:ENEURO.0317-20.2020. https://doi.org/10.1523/ENEURO.0317-20.2020.

[38] Shankar GM, Bloodgood BL, Townsend M, Walsh DM, Selkoe DJ, Sabatini BL. Natural

oligomers of the Alzheimer amyloid-beta protein induce reversible synapse loss by modulating an NMDA-type glutamate receptor-dependent signaling pathway. J Neurosci 2007;27:2866–75. https://doi.org/10.1523/JNEUROSCI.4970-06.2007.

[39] Scheff SW, Price DA, Schmitt FA, Mufson EJ. Hippocampal synaptic loss in early Alzheimer's disease and mild cognitive impairment. Neurobiol Aging 2006;27:1372–84. https://doi.org/10.1016/j.neurobiolaging.2005.09.012.

[40] Yuede CM, Lee H, Restivo JL, Davis TA, Hettinger JC, Wallace CE, et al. Rapid in vivo measurement of β-amyloid reveals biphasic clearance kinetics in an Alzheimer's mouse model. J Exp Med 2016;213:677–85. https://doi.org/10.1084/jem.20151428.

[41] Kayed R, Head E, Thompson JL, McIntire TM, Milton SC, Cotman CW, et al. Common structure of soluble amyloid oligomers implies common mechanism of pathogenesis. Science 2003;300:486–9. https://doi.org/10.1126/science.1079469.

[42] Savonenko A, Xu GM, Melnikova T, Morton JL, Gonzales V, Wong MPF, et al. Episodic-like memory deficits in the APPswe/PS1dE9 mouse model of Alzheimer's disease: relationships to beta-amyloid deposition and neurotransmitter abnormalities. Neurobiol Dis 2005;18:602–17. https://doi.org/10.1016/j.nbd.2004.10.022.

[43] Koffie RM, Meyer-Luehmann M, Hashimoto T, Adams KW, Mielke ML, Garcia-Alloza M, et al. Oligomeric amyloid beta associates with postsynaptic densities and correlates with excitatory synapse loss near senile plaques. Proc Natl Acad Sci U S A 2009;106:4012–7. https://doi.org/10.1073/pnas.0811698106.

[44] Koffie RM, Hashimoto T, Tai H-C, Kay KR, Serrano-Pozo A, Joyner D, et al. Apolipoprotein E4 effects in Alzheimer's disease are mediated by synaptotoxic oligomeric amyloid-β. Brain 2012;135:2155–68. https://doi.org/10.1093/brain/aws127.

[45] Faizi M, Bader PL, Saw N, Nguyen T-V V, Beraki S, Wyss-Coray T, et al. Thy1-hAPP(Lond/Swe+) mouse model of Alzheimer's disease displays broad behavioral deficits in sensorimotor, cognitive and social function. Brain Behav 2012;2:142–54. https://doi.org/10.1002/brb3.41.

[46] Yi B, Sahn JJ, Ardestani PM, Evans AK, Scott L, Chan JZ, et al. Small molecule modulator of sigma 2 receptor is neuroprotective and reduces cognitive deficits and neuro-inflammation in experimental models of Alzheimer's disease. J Neurochem 2017;140:561–75. https://doi.org/10.1111/jnc.13917.

[47] Zetterberg H, Blennow K. Neurogranin Levels in Cerebrospinal Fluid: A New Addition to the Alzheimer Disease Diagnostic Toolbox. JAMA Neurol 2015;72:1–3. https://doi.org/10.1001/jamaneurol.2015.2075.

[48] Kvartsberg H, Lashley T, Murray CE, Brinkmalm G, Cullen NC, Höglund K, et al. The intact postsynaptic protein neurogranin is reduced in brain tissue from patients with familial and sporadic Alzheimer's disease. Acta Neuropathol 2018. https://doi.org/10.1007/s00401-018-1910-3.

[49] Öhrfelt A, Brinkmalm A, Dumurgier J, Brinkmalm G, Hansson O, Zetterberg H, et al. The pre-synaptic vesicle protein synaptotagmin is a novel biomarker for Alzheimer's disease. Alzheimers Res Ther 2016;8:41. https://doi.org/10.1186/s13195-016-0208-8.

[50] Willemse EAJ, De Vos A, Herries EM, Andreasson U, Engelborghs S, van der Flier WM, et al. Neurogranin as Cerebrospinal Fluid Biomarker for Alzheimer Disease: An Assay Comparison Study. Clin Chem 2018;000:clinchem.2017.283028. https://doi.org/10.1373/clinchem.2017.283028.

[51] Portelius E, Zetterberg H, Skillbäck T, Törnqvist U, Andreasson U, Trojanowski JQ, et al. Cerebrospinal fluid neurogranin: relation to cognition and neurodegeneration in Alzheimer's disease. Brain 2015;138:3373–85. https://doi.org/10.1093/brain/awv267.

[52] Lleó A, Núñez-Llaves R, Alcolea D, Chiva C, Balateu-Paños D, Colom-Cadena M, et al. Changes in Synaptic Proteins Precede Neurodegeneration Markers in Preclinical Alzheimer's Disease Cerebrospinal Fluid. Mol Cell Proteomics 2019;18:546–60. https://doi.org/10.1074/mcp.RA118.001290.

[53] Higginbotham L, Ping L, Dammer E, Duong D, Zhou M, Gearing M, et al. Integrated Proteomics Reveals Brain-Based Cerebrospinal Fluid Biomarkers in Asymptomatic and Symptomatic Alzheimer's Disease (4738). Neurology 2020;94:4738. https://doi.org/10.1101/806752.

[54] Noble W, Hanger DP, Miller CCJ, Lovestone S. The importance of tau phosphorylation for neurodegenerative diseases. Front Neurol 2013;4 JUL:1–11. https://doi.org/10.3389/fneur.2013.00083.

[55] Scheltens P, Blennow K, Breteler MMB, de Strooper B, Frisoni GB, Salloway S, et al. Alzheimer's disease. Lancet (London, England) 2016;388:505–17. https://doi.org/10.1016/S0140-6736(15)01124-1.

[56] Gomez-Isla T. Neuronal Loss Correlates with but Exceeds Neurofibrillary Tangles in Alzheimer's Disease. Ann Neurol 1997;41:17–24.

[57] Serrano-Pozo A, Frosch MP, Masliah E, Hyman BT. Neuropathological alterations in Alzheimer disease. Cold Spring Harb Perspect Med 2011;1:a006189. https://doi.org/10.1101/cshperspect.a006189.

[58] Liu C, Song X, Nisbet R, Götz J. Co-immunoprecipitation with Tau isoform-specific antibodies reveals distinct protein interactions and highlights a putative role for 2N Tau in disease. J Biol Chem 2016;291:8173–88. https://doi.org/10.1074/jbc.M115.641902.

[59] Filtz TM, Vogel WK, Leid M. Regulation of transcription factor activity by interconnected, post-translational modifications. Trends Pharmacol Sci 2014;35:76–85.

[60] Saito S, Yamaguchi H, Higashimoto Y, Chao C, Xu Y, Fornace AJ, et al. Phosphorylation site interdependence of human p53 post-translational modifications in response to stress. J Biol Chem 2003;278:37536–44. https://doi.org/10.1074/jbc.M305135200.

[61] Russell CL, Mitra V, Hansson K, Blennow K, Gobom J, Zetterberg H, et al. Comprehensive Quantitative Profiling of Tau and Phosphorylated Tau Peptides in Cerebrospinal Fluid by Mass Spectrometry Provides New Biomarker Candidates. J Alzheimer's Dis 2016;55:303–13. https://doi.org/10.3233/JAD-160633.

[62] Dashinimaev EB, Artyuhov AS, Bolshakov AP, Vorotelyak EA, Vasiliev A V. Neurons Derived from Induced Pluripotent Stem Cells of Patients with Down Syndrome Reproduce Early Stages of Alzheimer's Disease Type Pathology in vitro. J Alzheimer's

Dis 2017;56:1–13. https://doi.org/10.3233/JAD-160945.

[63] Blennow K, Zetterberg H, Rinne JO, Salloway S, Wei J, Black R, et al. Effect of immunotherapy with bapineuzumab on cerebrospinal fluid biomarker levels in patients with mild to moderate Alzheimer disease. Arch Neurol 2012;69:1002–10. https://doi.org/10.1001/archneurol.2012.90.

[64] Mormino EC, Papp K V. Amyloid accumulation and cognitive decline in clinically normal older individuals: implications for aging and early Alzheimer's disease. J Alzheimers Dis 2018;64:S633–S646.

[65] Kumar D, Ganeshpurkar A, Kumar D, Modi G, Gupta SK, Singh SK. Secretase inhibitors for the treatment of Alzheimer's disease: Long road ahead. Eur J Med Chem 2018;148:436–52. https://doi.org/10.1016/j.ejmech.2018.02.035.

[66] Limegrover CSCS, LeVine III H, Izzo NJNJ, Yurko R, Mozzoni K, Rehak C, et al. Alzheimer's Protection Effect of A673T Mutation May Be Driven by Lower Aβ Oligomer Binding Affinity. J Neurochem 2020:in press. https://doi.org/10.1111/jnc.15212.

[67] Harper AR, Nayee S, Topol EJ. Protective alleles and modifier variants in human health and disease. Nat Rev Genet 2015;16:689–701. https://doi.org/10.1038/nrg4017.

[68] Yang T, Li S, Xu H, Walsh DM, Selkoe DJ. Large Soluble Oligomers of Amyloid β-Protein from Alzheimer Brain Are Far Less Neuroactive Than the Smaller Oligomers to Which They Dissociate. J Neurosci 2017;37:152–63. https://doi.org/10.1523/JNEUROSCI.1698-16.2017.

[69] Riad A, Lengyel-Zhand Z, Zeng C, Weng C-CC, Lee VM-YMY, Trojanowski JQ, et al. The Sigma-2 Receptor/TMEM97, PGRMC1, and LDL Receptor Complex Are Responsible for the Cellular Uptake of Aβ42 and Its Protein Aggregates. Mol Neurobiol 2020;57:3803–13. https://doi.org/10.1007/s12035-020-01988-1.

[70] Tarawneh R, D'Angelo G, Crimmins D, Herries E, Griest T, Fagan AM, et al. Diagnostic and Prognostic Utility of the Synaptic Marker Neurogranin in Alzheimer Disease. JAMA Neurol 2016;73:561–71. https://doi.org/10.1001/jamaneurol.2016.0086.

[71] Blennow K, Zetterberg H. Biomarkers for Alzheimer disease - current status and prospects for the future. J Intern Med 2018:0–2. https://doi.org/10.1111/joim.12816.

[72] Wellington H, Paterson RW, Portelius E, Törnqvist U, Magdalinou N, Fox NC, et al. Increased CSF neurogranin concentration is specific to Alzheimer disease. Neurology 2016;86:829–35. https://doi.org/10.1212/WNL.0000000000002423.

[73] Mairet-Coello G, Courchet J, Pieraut S, Courchet V, Maximov A, Polleux F, et al. The CAMKK2-AMPK Kinase Pathway Mediates the Synaptotoxic Effects of Aβ Oligomers through Tau Phosphorylation. Neuron 2013;78:94–108. https://doi.org/10.1016/j.neuron.2013.02.003.

[74] Crespo-Biel N, Theunis C, Borghgraef P, Lechat B, Devijver H, Maurin H, et al. Phosphorylation of protein Tau by GSK3β prolongs survival of bigenic Tau.P301L × GSK3β mice by delaying brainstem tauopathy. Neurobiol Dis 2014;67:119–32.

[75] Llorens-Martín M, Jurado J, Hernández F, Ávila J. GSK-3β, a pivotal kinase in Alzheimer disease. Front Mol Neurosci 2014.

[76] Mendoza J, Sekiya M, Taniguchi T, Iijima KM, Wang R, Ando K. Global analysis of phosphorylation of tau by the checkpoint kinases Chk1 and Chk2 in vitro. J Proteome Res 2013;12:2654–65. https://doi.org/10.1021/pr400008f.

[77] Ittner A, Chua SW, Bertz J, Volkerling A, van der Hoven J, Gladbach A, et al. Site-specific phosphorylation of tau inhibits amyloid-β toxicity in Alzheimer's mice. Science (80-) 2016;354:904–8. https://doi.org/10.1126/science.aah6205.

[78] Barthélemy NR, Mallipeddi N, Moiseyev P, Sato C, Bateman RJ. Tau phosphorylation rates measured by mass spectrometry differ in the intracellular brain vs. Extracellular cerebrospinal fluid compartments and are differentially affected by Alzheimer's disease. Front Aging Neurosci 2019;11:1–18. https://doi.org/10.3389/fnagi.2019.00121.

[79] Jarosz-Griffiths HH, Noble E, Rushworth J V., Hooper NM. Amyloid-β receptors: the good, the bad and the prion protein. J Biol Chem 2015:jbc.R115.702704. https://doi.org/10.1074/jbc.R115.702704.

[80] Hsieh H, Boehm J, Sato C, Iwatsubo T, Tomita T, Sisodia S, et al. AMPAR removal underlies Abeta-induced synaptic depression and dendritic spine loss. Neuron 2006;52:831–43. https://doi.org/10.1016/j.neuron.2006.10.035.

[81] Snyder EM, Nong Y, Almeida CG, Paul S, Moran T, Choi EY, et al. Regulation of NMDA receptor trafficking by amyloid-β. Nat Neurosci 2005;8:1051–8. https://doi.org/10.1038/nn1503.

[82] Ganapathy ME, Prasad PD, Huang W, Seth P, Leibach FH, Ganapathy V. Molecular and ligand-binding characterization of the sigma-receptor in the Jurkat human T lymphocyte cell line. J Pharmacol Exp Ther 1999;289:251–60.

[83] Klein WL. Abeta toxicity in Alzheimer's disease: globular oligomers (ADDLs) as new vaccine and drug targets. Neurochem Int 2002;41:345–52.

[84] Lambert MP, Viola KL, Chromy B a, Chang L, Morgan TE, Yu J, et al. Vaccination with soluble Abeta oligomers generates toxicity-neutralizing antibodies. J Neurochem 2001;79:595–605.

[85] Liu Y, Peterson D a, Schubert D. Amyloid beta peptide alters intracellular vesicle trafficking and cholesterol homeostasis. Proc Natl Acad Sci U S A 1998;95:13266–71.

[86] McDonald JM, Cairns NJ, Taylor-Reinwald L, Holtzman D, Walsh DM. The levels of water-soluble and triton-soluble Aβ are increased in Alzheimer's disease brain. Brain Res 2012;1450:138–47. https://doi.org/10.1016/j.brainres.2012.02.041.

[87] Schneider CA, Rasband WS, Eliceiri KW. NIH Image to ImageJ: 25 years of image analysis. Nat Methods 2012;9:671–5.

[88] Armstrong-James M, Millar J. Carbon fibre microelectrodes. J Neurosci Methods 1979;1:279–87.

[89] Portelius E, Olsson B, Höglund K, Cullen NC, Kvartsberg H, Andreasson U, et al. Cerebrospinal fluid neurogranin concentration in neurodegeneration: relation to clinical phenotypes and neuropathology. Acta Neuropathol 2018;136:363–76. https://doi.org/10.1007/s00401-018-1851-x.

[90] Brinkmalm A, Brinkmalm G, Honer WG, Frölich L, Hausner L, Minthon L, et al. SNAP-25 is a promising novel cerebrospinal fluid biomarker for synapse degeneration in Alzheimer's disease. Mol Neurodegener 2014;9:53. https://doi.org/10.1186/1750-1326-9-53.

[91] Croisé P, Houy S, Gand M, Lanoix J, Calco V, Tóth P, et al. Cdc42 and Rac1 activity is reduced in human pheochromocytoma and correlates with FARP1 and ARHGEF1 expression. Endocr Relat Cancer 2016;23:281–93. https://doi.org/10.1530/ERC-15-0502.

[92] Russell CL, Heslegrave A, Mitra V, Zetterberg H, Pocock JM, Ward MA, et al. Combined tissue and fluid proteomics with Tandem Mass Tags to identify low-abundance protein biomarkers of disease in peripheral body fluid: An Alzheimer's Disease case study. Rapid Commun Mass Spectrom 2017;31:153–9. https://doi.org/10.1002/rcm.7777.

[93] Johnson ECB, Dammer EB, Duong DM, Ping L, Zhou M, Yin L, et al. Large-scale proteomic analysis of Alzheimer's disease brain and cerebrospinal fluid reveals early changes in energy metabolism associated with microglia and astrocyte activation. Nat Med 2020. https://doi.org/10.1038/s41591-020-0815-6.

[94] Rankin CA, Sun Q, Gamblin TC. Tau phosphorylation by GSK-3ß promotes tangle-like filament morphology. Mol Neurodegener 2007;2:1–14. https://doi.org/10.1186/1750-1326-2-12.

[95] Salcedo-Tello P, Ortiz-Matamoros A, Arias C. GSK3 function in the brain during development, neuronal plasticity, and neurodegeneration. Int J Alzheimers Dis 2011;2011:7–10. https://doi.org/10.4061/2011/189728.

[96] Taus T, Köcher T, Pichler P, Paschke C, Schmidt A, Henrich C, et al. Universal and confident phosphorylation site localization using phosphoRS. J Proteome Res 2011;10:5354–62. https://doi.org/10.1021/pr200611n.

[97] Szklarczyk D, Gable AL, Lyon D, Junge A, Wyder S, Huerta-Cepas J, et al. STRING v11: Protein-protein association networks with increased coverage, supporting functional discovery in genome-wide experimental datasets. Nucleic Acids Res 2019;47:D607–13. https://doi.org/10.1093/nar/gky1131.

[98] LeVine H, Lampe L, Abdelmoti L, Augelli-Szafran CE, Le Vine H, Lampe L, et al. Dihydroxybenzoic acid isomers differentially dissociate soluble biotinyl-Aβ(1-42) oligomers. Biochemistry 2012;51:307–15. https://doi.org/10.1021/bi201288x.

[99] LeVine H. Biotin-avidin interaction-based screening assay for Alzheimer's beta-peptide oligomer inhibitors. Anal Biochem 2006;356:265–72. https://doi.org/10.1016/j.ab.2006.04.036.

[100] LeVine H, Ding Q, Walker JA, Voss RS, Augelli-Szafran CE. Clioquinol and other hydroxyquinoline derivatives inhibit Abeta(1-42) oligomer assembly. Neurosci Lett 2009;465:99–103. https://doi.org/10.1016/j.neulet.2009.08.002.

[101] Esparza TJ, Wildburger NC, Jiang H, Gangolli M, Cairns NJ, Bateman RJ, et al. Soluble Amyloid-beta Aggregates from Human Alzheimer's Disease Brains. Sci Rep 2016;6:38187. https://doi.org/10.1038/srep38187.

[102] Lleó A, Cavedo E, Parnetti L, Vanderstichele H, Herukka SK, Andreasen N, et al.

Cerebrospinal fluid biomarkers in trials for Alzheimer and Parkinson diseases. Nat Rev Neurol 2015;11:41–55. https://doi.org/10.1038/nrneurol.2014.232.

Acknowledgments: The authors wish to thank Dr. Hilary North Scheler for assistance with the preparation of this manuscript and Dr. Anthony Caggiano and Ms. Jennifer Iaci for their thoughtful review of the manuscript.

Funding: This work was supported by grants from the National Institute of Neurological Disorders and Stroke (NS080576 (HL) NS083175 (SC)), the National Institute on Aging (AG037337 (SC), AG055247 (SC), AG051593 (SC), AG054176 (SC)), the Alzheimer Drug Discovery Foundation (20100501 (SC)) and by Cognition Therapeutics.

Author contributions: N.I., C.Y. G.L, G.R., H.S., H.L., M.S., T.S., J.C. and S.C. designed the research. S.D., L.S., M.G. and S.C. designed the clinical trial and performed the clinical data analysis. C.Y., K.M.L., L.W., C.L, C.R., R.Y., C.H., H.L., M.S., D.C., T.S., and J.C. performed the research. N.I, C.Y., K.M.L., C.L., L.W., K.S., C.W., C.R., R.Y., G.L., G.R., C.H., H.L., M.S., T.S., J.C., D.C., M.H., and S.C. analyzed the data. N.I., S.C., and M.H. wrote the paper.

Competing interests: N.I., K.M.L., C.L., C.R., R.Y., L.W., G.L., G.R., H.S., M.H., C.W., K.S., and S.C. are employees of Cognition Therapeutics, Inc. CY, JC, HL, MS, MG and TS-J are paid consultants of Cognition Therapeutics, Inc. L.S. reports grants and personal fees from Eli Lilly, personal fees from Avraham, Ltd, personal fees from Boehringer Ingelheim, grants and personal fees from Merck, personal fees from Neurim, Ltd, personal fees from Neuronix, Ltd, personal fees from Cognition Therapeutics, Inc., personal fees from Eisai, personal fees from Takeda, personal fees from vTv, grants and personal fees from Roche/Genentech, grants from Biogen, grants from Novartis, personal fees from Abbott, grants from Biohaven, outside the submitted work. S.D. is a member of the Neuroscience Advisory Board for Amgen, Chair of the Medical Scientific Advisory Board for Acumen, Chair of the Drug Monitoring Committee for Biogen, Chair of the Medical Advisory Board for Cognition Therapeutics, Inc., and Editor for Dementia for UpToDate. H.Z. has served at scientific advisory boards for Cognition Therapeutics, Roche Diagnostics, Wave and Samumed, has given lectures in symposia sponsored by Biogen and Alzecure, and is a co-founder of Brain Biomarker Solutions in Gothenburg AB, a GU Ventures-based platform company at the University of Gothenburg. T.S. is a scientific advisory board member of Cognition Therapeutics, Inc. and receives collaborative grant funding from two pharmaceutical companies. K.B. has served as a consultant or at advisory boards for Alector, Biogen, Cognition Therapeutics, Lilly, MagQu, Novartis and Roche Diagnostics, and is a co-founder of Brain Biomarker Solutions in Gothenburg AB, a GU Venture-based platform company at the University of Gothenburg. International Patent WO 15/116923 pertains to the results presented in this paper.

Data and materials availability: All data needed to evaluate the conclusions in the paper are present in the paper itself and the Supplementary Materials or available upon request from the authors.

Figures

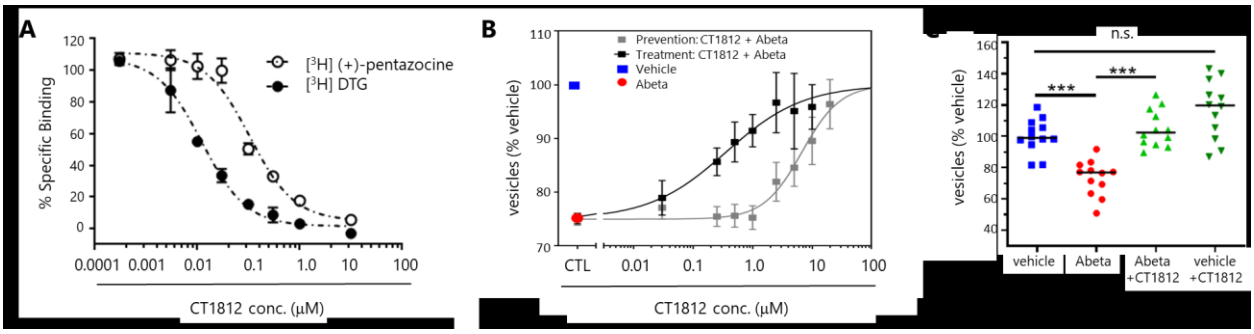

Fig. 1. CT1812 is a selective sigma-2 receptor ligand that prevents and treats Aβ oligomer-induced membrane trafficking deficits. (**A**) CT1812 binds sigma-2 receptors with a 8.5 nM Kd and sigma-1 receptors with a 63 nM Kd as measured in radioligand displacement studies (n=2; error bars = SD). (**B**) Effects of synthetic Aβ oligomers on vesicle trafficking in primary cultures of neurons and glia. Quantification is shown of the amount of formazan within intracellular vesicles in Aβ oligomer-treated (red dot) or vehicle-treated (blue square) conditions, and the dose-dependent restoration of trafficking rate to normal vehicle-treated values following CT1812 addition 1 hour before addition of Aβ oligomers (gray squares, EC50 = 6.7 μM, n = 11 experiments) or 1 hour after addition of Aβ oligomers (black squares, EC50 = 0.36 μM, n = 12 experiments). Vesicle trafficking was assayed 24 hours after addition of Aβ oligomers (1.75 μM, total peptide) (error bars = SEM). N represents the number of replicate experiments from separate cell culture preparations. (**C**) Human AD brain derived Aβ oligomers (1-hour treatment) caused a 27 ± 11% (SD) ($p < 0.001$, n=3) decrease in trafficking rate in cultured neurons and glia. Pretreatment of cultures for 1 hour with 15 μM CT1812 before addition of human derived Aβ oligomers blocked the trafficking deficits ($p < 0.001$ for Aβ Oligomers vs. Aβ Oligomers + CT1812, ANOVA with Tukey's post hoc test, n = 3 experiments). Each point represents results from quadruplicate replicates from Aβ oligomer preparations isolated from three separate donor brains.

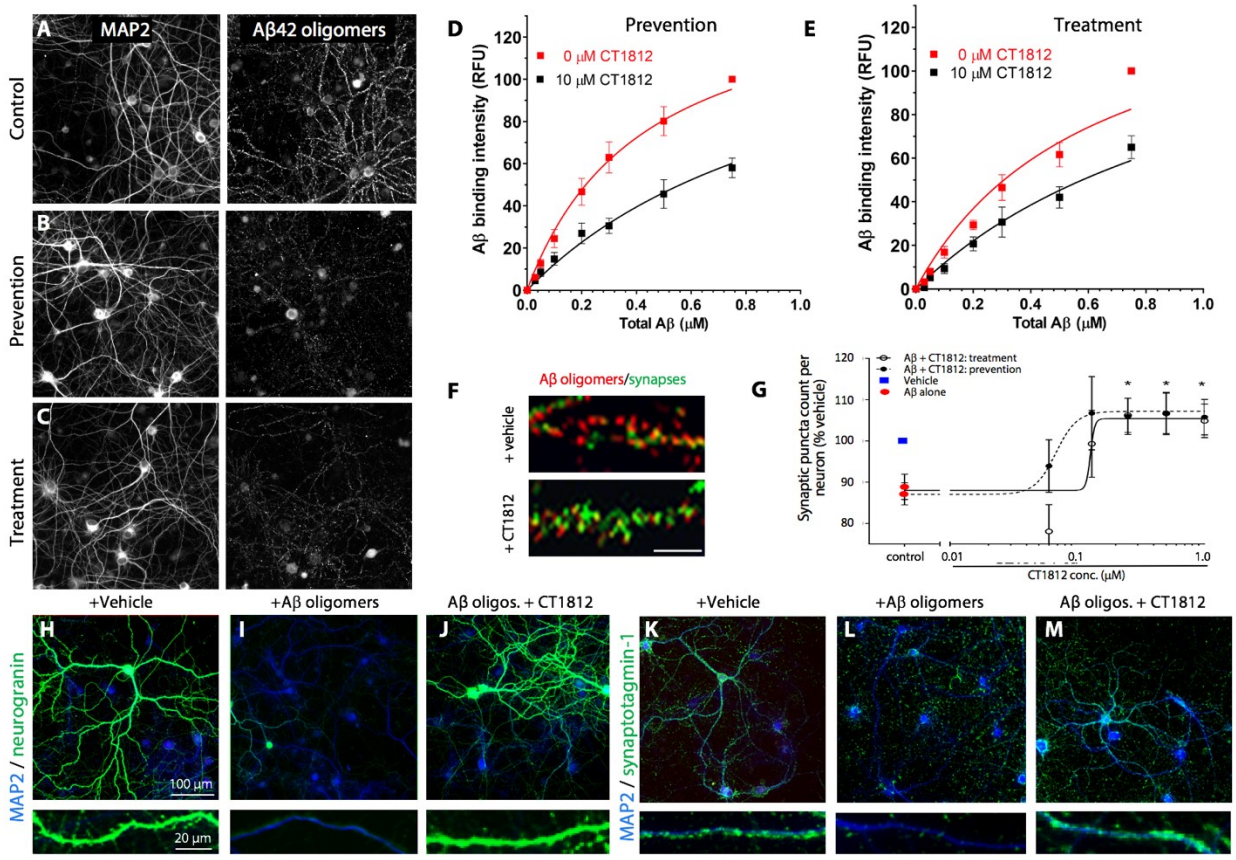

Fig. 2. **CT1812 prevents Aβ oligomer binding to and displaces bound oligomers from neuronal receptors, leading to restoration of synaptic density and protein expression in cultured mouse neurons.** (**A**) Aβ oligomers (750 nM, >80% of Kd) bind specifically and saturably to a single receptor site on some, but not all, neurons in mature (>21 DIV) primary hippocampal and cortical neuronal cultures. (**B**) CT1812 [10 uM] prevents Aβ binding by 59 ± 8% (SEM) when added 1 hour prior to addition of Aβ oligomers. (**C**) CT1812 [10 uM] displaces Aβ oligomer binding by 42 ± 9% (SEM) when added 1 hour after addition of Aβ oligomers. Scale bar = 20 microns. (**D**) CT1812 prevents binding and more than doubles the Kd of oligomer binding, from 430 nM (at 0 μM CT1812) to 1120 nM (at 10 μM CT1812) (n=6; error bars = SEM). (**E**) CT1812 displaces binding and nearly doubles the Kd of oligomer binding, from 610 nM (at 0 μM CT1812) to 1160 nM (for 10 μM CT1812) (n=6; error bars = SEM). (**F, top**) Aβ oligomers bind to receptors at neuronal synapses (red, 6E10 immunodetection), resulting in a significant loss of synapses (green, drebrin immunodetection, 12.8 ± 2.6% (SEM) decrease in synapse density, $p<0.01$ vs. vehicle-treated, Student's t-test [**G**]; the blue square represents synapse density in vehicle-treated neurons.) (**F, bottom**) CT1812 displaces bound Aβ oligomers and restores synaptic numbers to normal in a dose-dependent manner. Scale bar = 5 microns. (**G**) CT1812 restores synapse number to normal whether added before (prevention, EC50 = 68 nM) or after (treatment, EC50 = 127nM) Aβ oligomers (*$p<0.5$ vs. Aβ oligomers alone for both conditions, Student's t-test, error bars = SEM). Treatment with CT1812 restores synaptic protein expression in cultured rat neurons**.** (**H**) Neurogranin is expressed at high levels in postsynaptic dendrites and synapses in a subset of neurons in primary hippocampal/cortical cultures. (**I**) Addition of Aβ oligomers (0.75 μM, 24 hours) cause a 28% loss of neurons expressing high

levels of neurogranin ($p = 0.014$). (**J**) Treatment with 4.8 μM CT1812 1 hr after addition of Aβ oligomers restores the expression of neurogranin to normal levels (Aβ oligomers vs. Aβ oligomers + CT1812 $p = 0.031$, vehicle vs. Aβ oligomers + CT1812, n.s., ANOVA with Tukey's post hoc test, $n = 20$). (**K**) Synaptotagmin-1 is expressed in presynaptic terminals. (**L**) Addition of Aβ oligomers (3.5 μM, 48 hours) cause a 37% loss of synaptotagmin-1 presynaptic terminals in primary hippocampal/cortical cultures ($p = 0.0068$, $N = 24$) (**M**) Treatment with 4.8 μM CT1812 1 hr after addition of Aβ oligomers blocks these losses and restores expression of synaptotagmin-1 levels (vehicle vs. Aβ oligomers + CT1812, n.s). (**H-M**) ANOVA with Tukey's post hoc test, $n = 20$. For all cell culture experiments, n represents the number of replicate experiments from separate cell culture preparations, and data points represent means ± SD or SEM as noted.

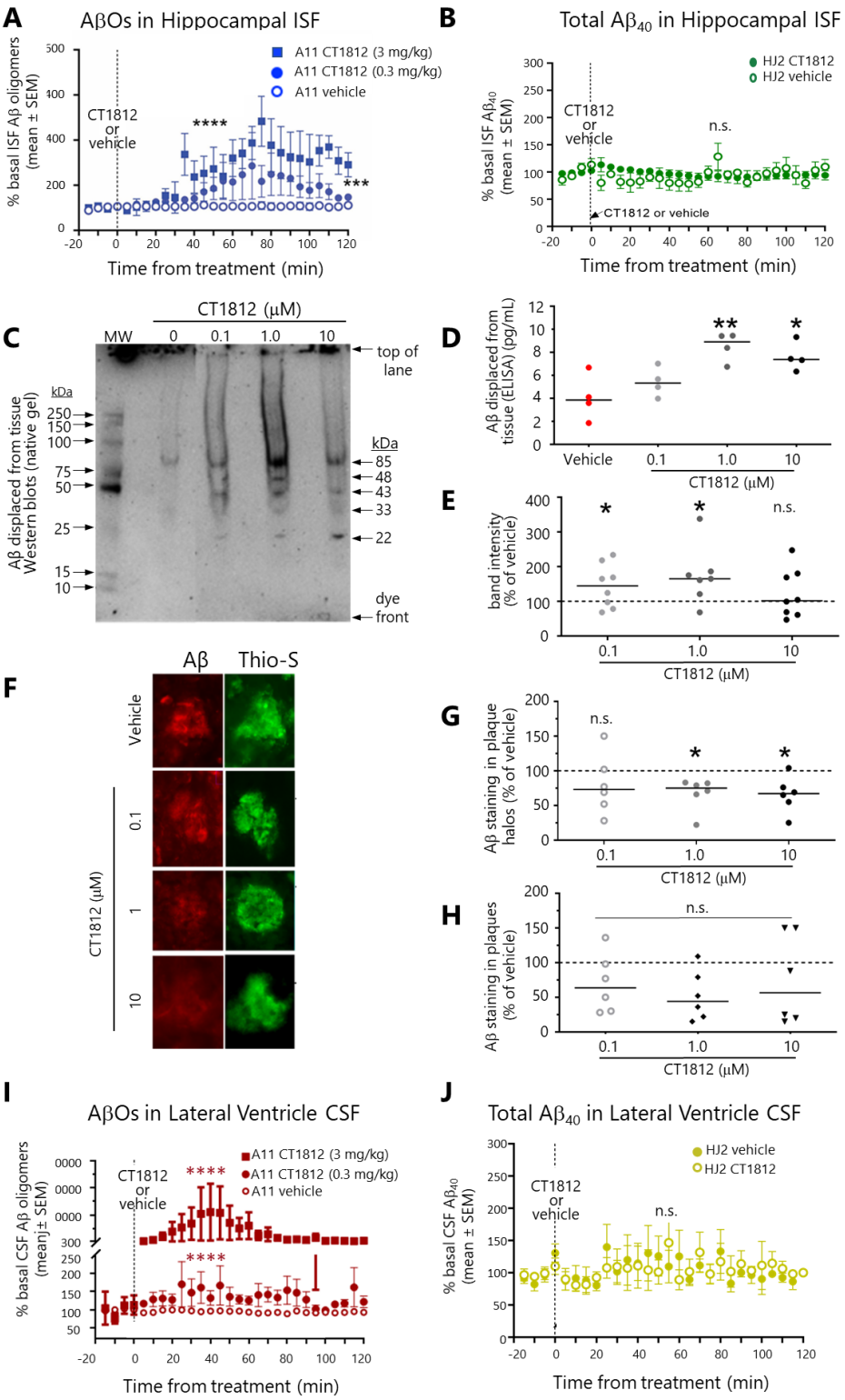

Fig 3. CT1812 treatment displaces Aβ oligomers from mouse hippocampal receptors and postmortem AD human patient tissue and facilitates their clearance into CSF. (A, B) Microimmunoelectrodes (MIE) coated with oligomer-specific antibody A11 (**A**) or mAβ40

antibody HJ2 (**B**) in 12-month-old transgenic hAPP/PS1 mice detect soluble Aβ in the hippocampal interstitial fluid (ISF). (**A)** Following i.v. injection of 0.3 or 3 mg/kg CT1812 (vertical dashed line), soluble Aβ oligomers are significantly elevated in hippocampal ISF in CT1812-treated mice (n=7) compared to vehicle-treated mice (n=4, *** p< 0.001, **** p<0.0001, two-way ANOVA with Sidak's post hoc test for effect of drug vs. vehicle.) (**B**) CT1812 treatment does not cause a change in total Aβ levels in the hippocampus (n=5) compared to vehicle treatment (n=4). (**C-E**) Aβ oligomers displaced from post-mortem brain tissue sections from 8 AD patients were quantified by ELISA (**D**) and native western blots (**C** [representative individual patient]**, E**), and show the expected dose-dependent increase in concentration in CT1812-treated compared to the vehicle-treated condition. For western blots, the sum of the intensity of discrete Aβ protein bands at 22, 33, 43, 48 and 85 Kd was quantified for each donor tissue section (**C**). In (**D**) and (**E**), values for Aβ measured by ELISA for each brain tissue section and for intensity of western blot bands for each brain tissue section normalized to vehicle-treated controls (dashed line) from the same donor are shown (*p < 0.05, ANOVA with Tukey's post hoc test for each treatment vs vehicle treated controls). (**F** [representative individual patient]**, G, H**) Aβ oligomers (red) located in a 2 μM halo surrounding compact thioflavin-S positive plaques (green) are displaced from frozen postmortem human AD brain tissue sections (N=5 patients) by CT1812 in a dose-dependent manner normalized to vehicle treated brain sections (dashed line) from the same individual (*p < 0.05, ANOVA with Tukey's post hoc test for each CT1812-treated vs vehicle-treated controls). (**H**) Aβ intensity within plaques does not change. Scale bar = 20 μM. (**I, J**) Microimmunoelectrodes coated with oligomer-specific antibody A11 (**I**) or pan-Aβ antibody HJ2 (**J**) in 12 month old transgenic hAPP/PS1 mice detect soluble Aβ in the lateral ventricle cerebrospinal fluid (CSF). (**I**) Following i.v. injection of 0.3 (n=7) or 3 (n=5) mg/kg CT1812 (vertical dashed line), soluble Aβ oligomers are significantly elevated in lateral ventricle CSF compared to vehicle-treated mice (n=5). (**J**) CT1812 treatment (n=5) did not cause a change in Aβ monomer levels in the CSF compared to vehicle treatment (n=4). *** p< 0.001, **** p<0.0001, two-way ANOVA Sidak's post hoc test for effect of drug vs. vehicle.

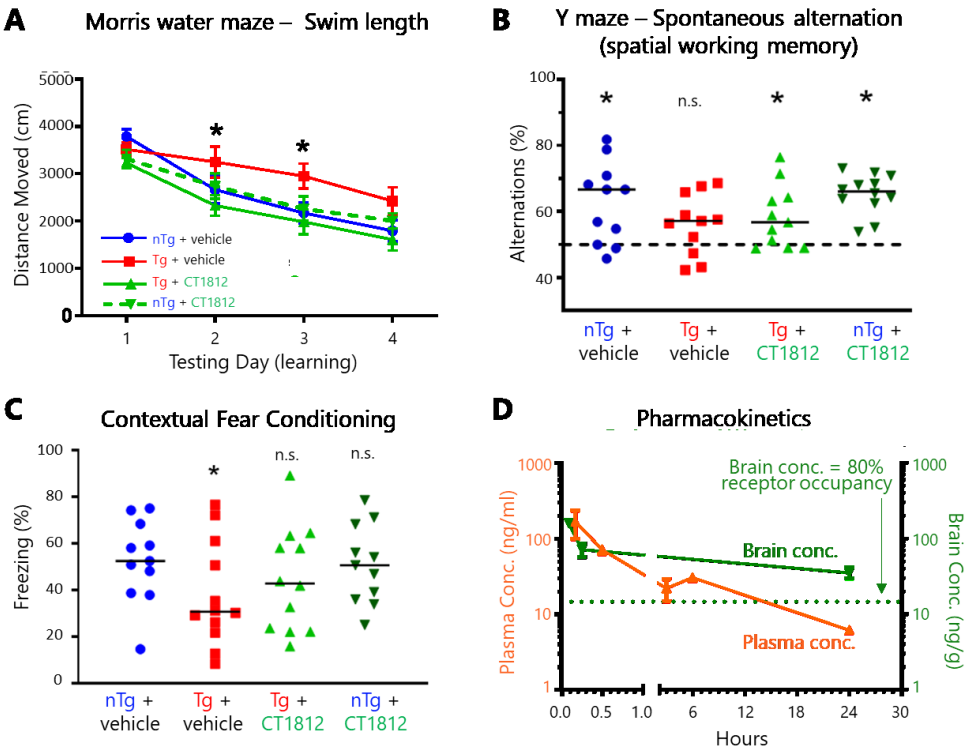

Fig. 4. Treatment with CT1812 improves learning and memory deficits in transgenic Alzheimer's mice. (**A**) Transgenic Thy-1 huAPPSwe/Ldn+ male mice treated with CT1812 (Tg + CT1812) learn the Morris water maze task significantly better than do transgenic vehicle-treated mice (Tg + vehicle; p=0.016, two-way repeated measures ANOVA, Bonferroni post hoc *p < 0.5; error bars = SEM). CT1812 treatment does not affect non-transgenic animal performance (nTg + CT1812). (**B**) Transgenic mice treated with CT1812 remember previous arms entered in the Y maze task significantly better (p=0.013, Student's t test) than chance (dashed line), but transgenic vehicle-treated animals do not (nTg + vehicle, 62.7 ± SD 12.2%; Tg + vehicle, 56.1 ± SD 9.2%; Tg + CT1812, 58.5 ± SD 9.4%; nTg + CT1812, 65.3 ± SD 6.0%). (**C**) Transgenic mice show deficits in the Contextual Fear Conditioning test (p = 0.037, Student's t-test), while transgenic and non-transgenic mice treated with CT1812 do not (nTg + vehicle, 52.5 ± SD 5.4%; Tg + vehicle, 37.9 ± SD 6.4%; Tg + CT1812, 44.6 ± SD 6.5%; nTg + CT1812, 50.9 ± SD 5.1%). (Each data point represents an individual mouse.) (**D**) Plasma and brain concentration of CT1812 following a single p.o. dose of 10 mg/kg.

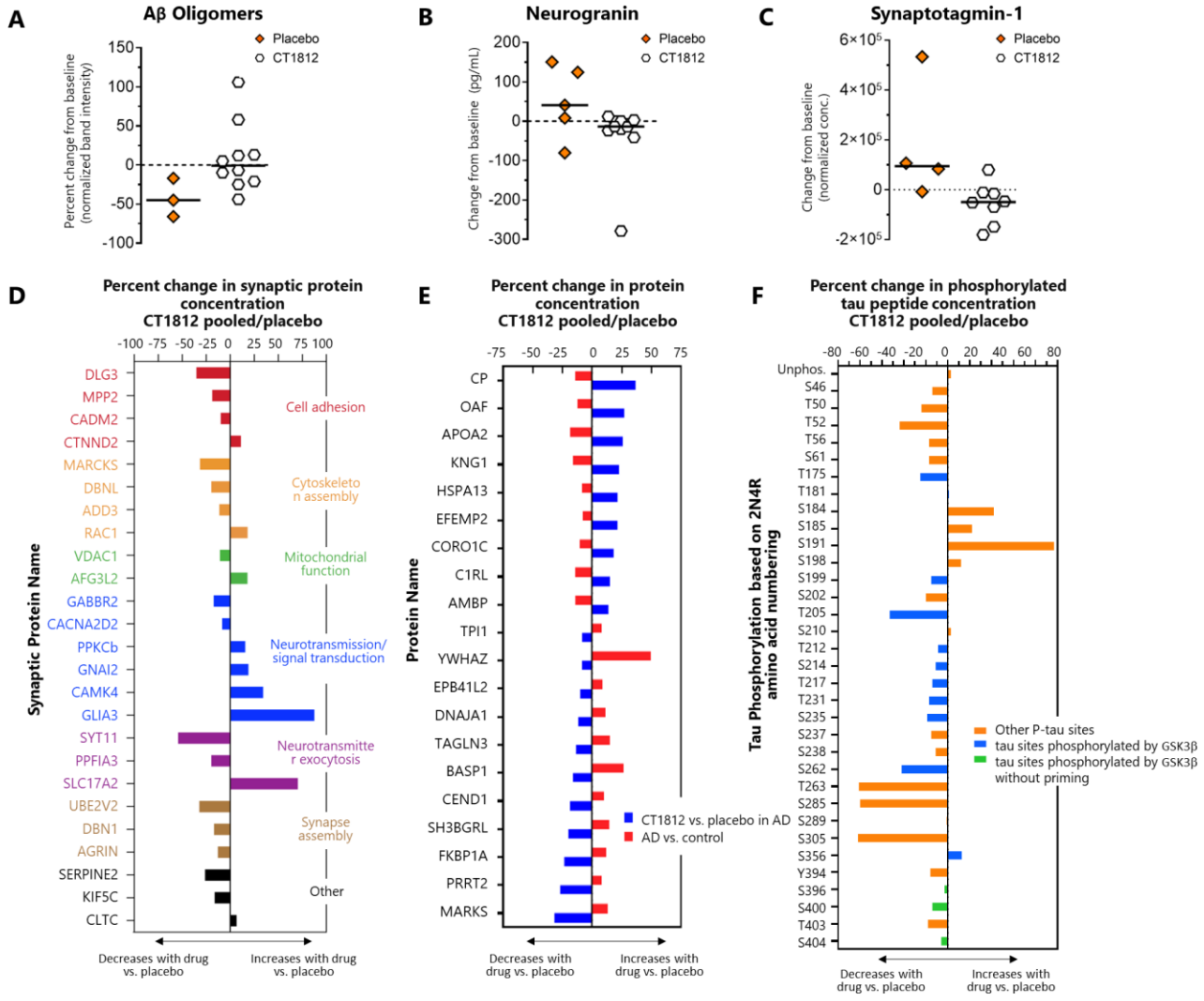

Fig. 5. CT1812 treatment significantly impacts CSF biomarkers of target engagement and disease-related biology. Protein concentrations in CSF samples from AD patients in a 28 day phase 1b/2a clinical trial of CT1812 vs. placebo were measured via ELISA, LC-MS/MS or gel electrophoresis. (**A**) After 28 days the concentration of Aβ oligomers measured via western blot in CT1812-treated AD patient CSF increases compared to the patient's own baseline and vs. placebo (p=0.014, Student's t test, n = 3 placebo, 10 CT1812-treated), providing supporting evidence of clinical target engagement. At day 28 of the study, the concentration of synaptic damage proteins neurogranin (**B**, measured by ELISA) and synaptotagmin-1 (**C**, measured by LC-MS/MS) decreases compared to the patient's own baseline and vs. placebo (p=0.050 ANCOVA, n = 5 placebo, 11 CT1812-treated; and F1,12 = 8.8, p = 0.011, n = 4 placebo, 9 CT1812-treated, respectively) providing evidence of a positive effect on synapses in patients with AD. (**A**, **B** and **C**) Data from individual patients are displayed. These changes are corroborated (**D**) by significant expression changes (p<0.05) in multiple synaptic proteome proteins in the CSF measured by unbiased LC-MS/MS in AD patients treated for 28 days with CT1812 vs. placebo. (**E**) CSF Proteomics identifies a subset of proteins significantly altered with CT1812 that have been reported to be significantly regulated in AD [93]. Data are expressed as

mean % change in protein concentration in CSF from CT1812 treated (n=11) versus placebo (n=4) (blue) and AD versus control to illustrate how these proteins are altered in AD relative to cognitively normal age-matched controls. All analytes shown are significantly regulated ($p<0.05$) in AD patients vs. control [53] and in the present study. (**F**) Following 28 days of treatment, the abundance of six tau phosphorylation peptides decreased by 30% (the threshold for noise distribution), or more after treatment with CT1812 compared to placebo (T52, T205, S262, S263, S285, S305) while one site increased more than 30% (S191), but the concentration of unphosphorylated tau did not change, providing evidence of CT1812 impact on pathological disease signaling. Colored bars represent amino acid sites within tau that are phosphorylated by GSK3β with priming (blue bars) or without priming (green bars) [94,95].

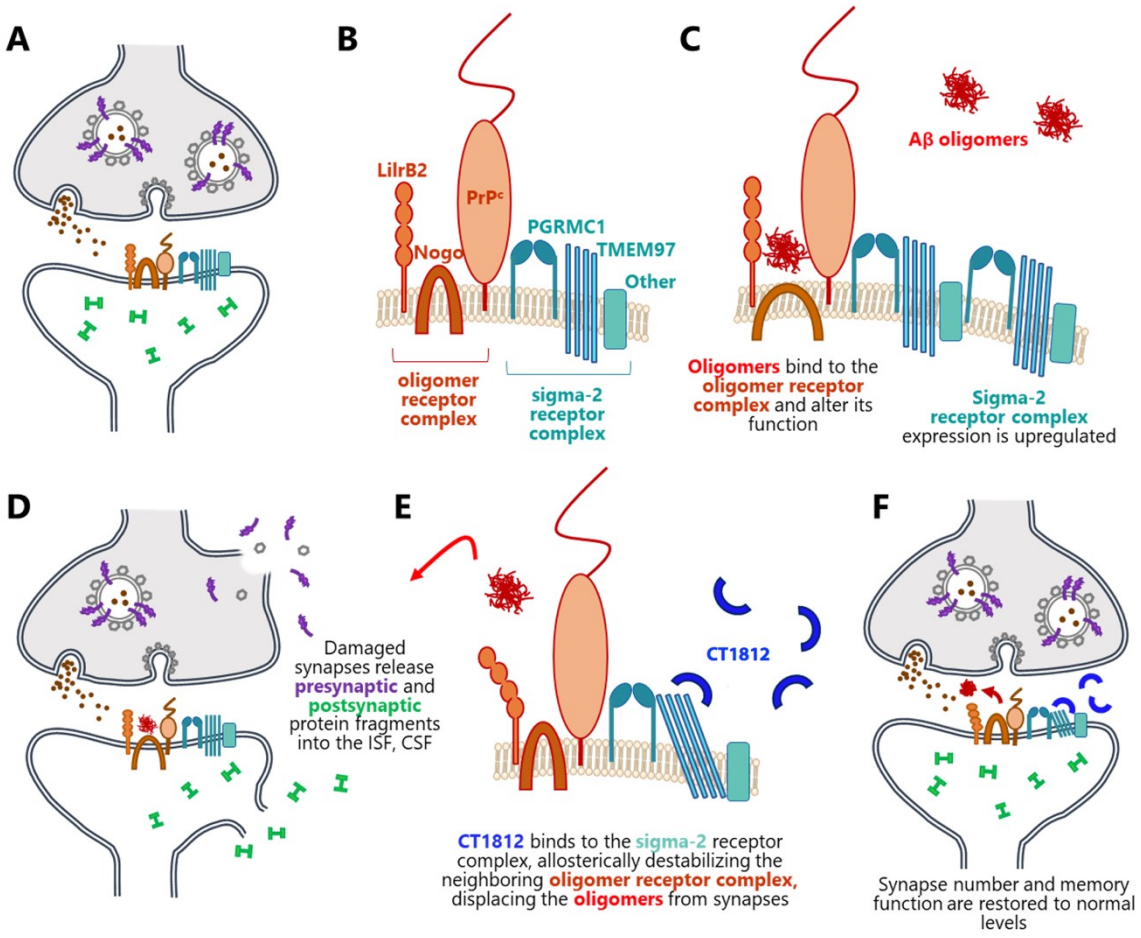

Fig. 6. Hypothesized mechanism of action of CT1812: synaptoprotective displacement of toxic Aβ oligomers from neurons. (A) In the absence of Aβ oligomers, pre- and post-synaptic proteins such as synaptotagmin-1 and neurogranin are expressed at normal levels. **(B)** The sigma-2 receptor complex tightly regulates the oligomer receptor complex by stabilizing plasma membrane expression of oligomer receptor component proteins. **(C)** Oligomer binding results in changing expression/localization of synapse associated proteins, spine loss, and memory failure, as well as upregulation of the sigma-2 receptor complex. **(D)** Fragmented pre- and post-synaptic proteins such as synaptotagmin-1 and neurogranin move into ISF and then CSF. **(E)** CT1812 binds to the sigma-2 receptor ligand binding site within the sigma-2 receptor complex, acting as a negative allosteric modulator of Aβ oligomer binding. This destabilizes the oligomer binding site and displaces oligomers from synapses without affecting normal synapse protein function. **(F)** Synapse number and memory are restored to normal levels.

Supplementary Materials and Methods

MIE preparation

A single length of carbon fiber (5μm diameter, GoodFellow Corp, England) was aspirated into a glass capillary tube (0.4 mm inner diameter, 4" length, A-M Systems, WA, USA), pulled using a pipette puller (Narishige PE-22, Japan) and attached to an insulated silver wire using conductive silver adhesive paste (Ted Pella, CA, USA). The junction between the wire and the glass capillary tube was sealed using heat shrink tubing (NTE Electronics, NJ, USA). The carbon fiber was cut to a length of 30-60 μm. To enhance binding of the capture antibody, the microelectrodes were pretreated using a triangular waveform from 0 to 3V for 20 s, held at -0.8 V for 5 sec, and then held at 1.5 V for 10 sec in PBS. Activation of carboxylic groups on the carbon fiber surface was achieved by application of 0.4 M of EDC and 0.1 M of NHSS solutions (Thermo Scientific, IL, USA) to form a semi-stable reactive amine NHS ester. The activated microelectrodes were placed in a solution of 10 ug/ml A11 antibody (Invitrogen, Rockford, IL, USA) or HJ2 (Washington University, St. Louis, USA) and incubated at room temp for 10 min and then 4 °C overnight. Following antibody attachment, MIEs were incubated with 0.05% ethanolamine to deactivate reactive amine sites then 1% BSA to block non-specific protein binding sites.

In vitro calibration of the MIEs

In vitro calibration of the MIEs before experiments were conducted using a CH Instruments 660D Electrochemical Workstation with PicoAmp booster (CH Instruments Inc, TX, USA). A conventional three-electrode cell consisting of an Ag/AgCl reference electrode (1M KCL), and a platinum wire as a counter electrode was used in all experimental procedures. Oligomers were prepared by incubating 100 uM synthetic human Aβ42 (American Peptide Co, CA, USA) 1:50 in 10 mM HCl, 150 mM NaCl in ddH2O at 4C for 16 hours. Calibration curve concentrations were prepared in 5-fold serial dilutions ranging from 16 pg/ml to .204 fg/ml in 1% BSA for Aβ oligomers, and from 200 ng/ml to 512 fg/ml for Aβ monomers. Square Wave Voltammetry (SWV) was used to monitor the response of the electrode in different concentrations of Aβ oligomers. SWV parameters used were: Init E (V) = 0; Final E (V) = 1.2; Incr E (V) = 0.004; Amplitude (V) = 0.04; Frequency (Hz) = 15.

In vivo MIE experiments

The APP/PS1 mice used in these experiments contain a PS1ΔE9 mutation and human APP Swedish mutation that were inserted into a single locus. Animals were screened for the PS1 and APP transgenes by polymerase chain reaction from tail DNA. All electrodes used for MIE studies were calibrated against known concentrations of Aβ oligomers prior to the experiment, and only MIEs showing increasing response to increasing concentrations of Aβ oligomers in vitro were used for in vivo experiments. MIEs were inserted into the hippocampus at coordinates: A/P -3.1 mm, M/L 2.6 mm, and D/V -1.7 mm, or into the lateral ventricle at coordinates: A/P -0.6 mm, M/L 1.2 mm, and D/V -1.6 mm.

Statistical analysis of MIE experiments

All in vitro measurements were carried out in triplicate and the average of the three SWV scans was used for analysis. All current responses recorded were subtracted from background and fit to baseline for peak analysis using CH Instruments software. Results are expressed as mean ± SEM

Differences in clearance rates between groups were analyzed in GraphPad Prism software using T-tests, and Repeated Measures ANOVA with Bonferroni post hoc tests were used to analyze percent changes in baseline levels over time. Statistical significance in all analyses was set at $p < 0.05$.

Combined tissue and CSF analysis of synaptic proteins and phosphorylated tau

Tissue-enhanced analysis of CSF protein expression was performed using TMTcalibrator™. CSF samples were provided under partially blinded conditions: samples were grouped according to treatment type, but the identity of the placebo- or drug-treated group was undisclosed. Frozen brain tissue from three regions (frontal, parietal cortices and cingulate gyrus) from the same post-mortem brain (Caucasian, female, 67 years old, APOE E3/E4), confirmed as being Braak Stage IV-VI (Bielchowski silver stain) with abundant neuritic plaques and neurofibrillary tangles, were purchased from BioIVT (Burgess Hill, UK) for use as the calibrant/trigger. Approximately 500 mg of each brain tissue was lysed (8M urea, 75 mM NaCl, 80 mM Tris; pH 8.2 containing phosphatase and protease inhibitors). Tissue debris was removed by centrifugation at 12000g, 4°C for 2x10 min and supernatants containing 27 mg total protein from each lysate were pooled, diluted to a concentration of 3 mg/ml, aliquoted and stored at -80°C.

For each TMT® 11plex eight individual CSF samples containing 150 µg total protein along with three replicate aliquots of 700 µg total protein of the brain lysate were processed in parallel. Proteins were denatured in 100 mM tetraethylammonium bromide (TEAB) buffer and 0.1% sodium dodecyl sulfate (SDS), reduced with 1 mM tris (2- carboxyethyl) phosphine (TCEP) and incubation at 55°C for 60 min, and finally alkylated with 7.5 mM iodoacetamide at room temperature for 60 min. Proteins were digested overnight at 37°C in ~1:25 ratio trypsin to total protein weight and subsequently labeled using TMT® 11plex reagents (15 mM), incubated at room temperature for 1 hour, and quenched by the addition of 0.25% hydroxylamine for 15 min. Each of the 11 individual TMT® labelled samples (8 x CSF, 3 x brain) were the pooled to form the analytical TMT® 11plex sample. For further processing, each TMT® 11plex sample was split into aliquots of 1 x 50 µg (quality control), 2 x 100 µg (total protein analysis) and 1 x 3,050 µg (phosphoproteomics).

Phosphopeptide Enrichment: Each TMT® 11plex sample (~3050 µg) was enriched for phosphopeptides using the High Select™ FeNTA Phosphopeptide Enrichment Kit (Thermo Scientific Pierce, cat. no. A32992) according to manufacturer`s instructions.

Basic Reversed-Phase Fractionation: Basic reversed-phase (bRP) fractionation was conducted in parallel for both non-enriched peptides the enriched phosphopeptides from each TMT® 11plex using Pierce™ High pH Reversed-Phase Peptide Fractionation Kit (Thermo Scientific, cat. no. 84868) according to manufacturer`s instructions and six individual fractions produced for each of the non-enriched and phosphopeptide enriched .

Liquid Chromatography Tandem Mass Spectrometry (LC-MS/MS): The 12 bRP fractions were analysed by LC-MS/MS using the EASY-nLC 1000 system coupled to an Orbitrap Fusion™ Tribrid™ Mass Spectrometer (both Thermo Scientific). Re-suspended peptides were loaded onto a nanoViper C18 Acclaim PepMap 100 pre-column (Thermo Scientific) and resolved using an increasing gradient of acetonitrile in 0.1% Formic acid through a 50 cm PepMap RSLC analytical column (Thermo Scientific) at a flow rate of 200 nL/min. LC gradient started with 10% ACN up to 30% ACN over 160min and was increased to 90% ACN over 10min at a flow rate of 300nL/min. Peptide mass spectra were acquired throughout the entire chromatographic

run (180 minutes), using top speed higher collision induced dissociation (HCD) Fourier-transform mass spectrometry (FTMS) MS2 scans at 60,000 resolving power @ 400 mass over charge (m/z), following each FTMS scan (120,000 resolving power @ 400 m/z).

Computational Mass Spectrometry: In total 64 separate raw files were submitted to Proteome Discoverer (PD) v2.1 (Thermo Scientific) using the Spectrum Files node. The Spectrum Selector was set to its default values while the SEQUEST HT node was suitably set up to search data against the human FASTA UniProtKB/SwissProt database (version November 2018). Up to ten sequence matches per spectrum were permitted. The reporter ions quantifier node was set up to measure the raw intensity values for TMT® 11plex mono-isotopic ions (126, 127N, 127C, 128N, 128C, 129N, 129C, 130N, 130C, 131, 131C). The SEQUEST HT search engine was programmed to search for tryptic peptides (with two missed cleavages) and with static modifications of carbamidomethyl (C), TMT6plex (K), and TMT6plex (NTerm). Dynamic modifications were set to phosphorylation (STY), deamidation (N/Q) and oxidation (M). Precursor mass tolerance was set to 20 parts per million (ppm) and fragment (b and y ions) mass tolerance to 0.02Da. Spectra were also searched using the ptmRS-2.0 (fragment mass tolerance of 0.02Da, considering neutral loss peaks for collision induced dissociation (CID) and HCD) and Percolator nodes. The ptmRS node scored each phosphate group (assigned to serine, threonine or tyrosine residues) with a local site confidence probability score within each phosphorylated peptide sequence. A score greater than or equal to 75% was considered as an unambiguous site assignment, while scores less than 75% were considered ambiguous [96]. All raw intensity values were exported to tab delimited text files for later processing and filtering using in-house software. Grouped protein results were exported to tab-delimited "Multi-consensus.txt files", filtered at 1% false discovery rate (FDR) (PSM level) and 1 x Rank 1 peptide per protein. Protein grouping was performed using the Parsimony Principle option in the Protein Grouping area within PD. More information about the protein grouping algorithm can be found in the Proteome Discoverer (PD) Version 2.1 User Guide (version A, July 2015). Results were filtered at 1% FDR (PSM level and Protein level) and exported to tab-delimited "Multi-consensus.txt files."

Graphical outputs and final table of results were produced using a selection of automated scripts that had been written in R. The log2 ratio (AD group median CSF signal intensity divided by the control group median CSF signal intensity) was graphed as a percent difference. The noise distribution cutoff was determined to be 30% (up- or down-regulation).

For visualizaton of phospho-site inter-relationships, hierarchical clustering (Pearson) was performed for both rows and columns using Average Linkage using https://software.broadinstitute.org/morpheus/.

Pathway analysis was performed using IPA (v51963813, QIAGEN Inc., https://www.qiagenbioinformatics.com/products/ingenuitypathway-analysis), Metacore (v19.4 build 69900, and STRING (v11] [97].

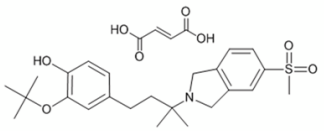

CT1812 Fumarate

Target	Cerep/Eurofins Catalog number	Assay type	Binding Ki (nM)
Sigma-2	0148	Radioligand binding	8.5
Sigma-1	0889	Radioligand binding	63

Binding Activity > 1,000 nM

Target	Catalog No.	Target	Catalog No.	Target	Catalog No.
M1	091	NK3	0104	CAMK4	1582
M2	093	Y1	0106	CDK/p35	2877
M3	095	Y2	0107	EGFR kinase	2865
Ca^{+2} Channel	0163	NTS1	0109	EphA4 kinase	1702
NE Transporter	0355	Kapa opioid	1971	EphB2 kinase	3054
DA transporter	0052	Delta 2 opioid	0114	EphB4 kinase	3059
5-HT transporter	0439	Mu Opioid	0118	FAK	3065
Adenosine Transporter	0007	N Opioid	0358	Choline Transporter	1552
Adenosine 1	0002	Sst	0149	FGFR1 kinase	2868
Adenosine A2A	0004	VPAC1	0157	FGFR3 kinase	2894
AdenosineA3	0006	V1a	0159	FGFR4 kinase	2895
ATP1	0024	Kv channel	0166	Fyn kinase	0212
BZD	0028	SKCa channel	0167	HER/ErbB2 kinase	1598
B2	0033	Cl channel	0170	IGF1R	3061
CB1	0036	AMPA	0064	IRK	2898
CCK1	0039	GABA Transporter	0060	GSK3β	2879
ETA	0054	NMDA	0066	PKA	2927
GABA	0057	Glycine	0068	PKCα	0348
CXCR2	0419	N α4β2	3029	PKCβ1	2888
GAL2	0410	N α7	3010	PKCβ2	2750
CCR1	0361	PCP	0124	PKCγ	0350
H1	0870	NMDA	0066	RAF-1 kinase	2936
H2	1208	Kainate	0065	Src kinase	2907
MC4	0420	AMPKinaseα	1572	mTOR kinase	2941
MT1	1538	CAMK1α	2739	TRKA	2901
NK2	0102	CAMK2α	3024	Na+ Channel (site2)	0169

Activity EC50 > 1,000 nM

Target	Catalog No.	Target	Catalog No.	Target	Catalog No.
alpha 1A (agonist)	1500	5HT2A (agonist)	1023	D1 (antagonist)	1686
alpha 1B (agonist)	1901	5HT2B (agonist)	1377	D3 (antagonist)	684
alpha 2A agonist)	2558	5HT2C (agonist)	1221	D2S (antagonist)	2569
alpha 2B (agonist)	1813	5HT4e (agonist)	1044	D4.4 (antagonist)	684
alpha 2C (agonist)	1736	5HT6 (agonist)	1627	5HT1 A (antagonist)	2101
Beta1 (agonist)	1605	5HT7 (agonist)	1661	5HT1B (antagonist)	2604
Beta 2 (agonist)	1976	alpha 1A (antagonist)	1501	5HT2A (antagonist)	1024
Beta 3 (agonist)	2189	alpha 1B (antagonist)	1902	5HT2B (antagonist)	1812
D1 (agonist)	1685	alpha 2A (antagonist)	2559	5HT2C (antagonist)	3199
D2S (agonist)	2566	alpha 2B (antagonist)	1814	5HT4e (antagonist)	1045
D3 (agonist)	0683	alpha 2C (antagonist)	1737	5HT6 (antagonist)	1628
D4.4 (agonist)	1699	Beta1 (antagonist)	1606	5HT7 (antagonist)	1662
5HT1A (agonist)	2093	Beta 2 (antagonist)	1977		
5HT1B (agonist)	2600	Beta 3 (antagonist)	2191		

Supplementary Fig. 1 Counterscreening reveals that CT1812 is a selective sigma-2 ligand. Structure of CT1812 fumarate is shown. CT1812 is 100-fold selective for sigma-2 receptors vs. 72 other receptors.

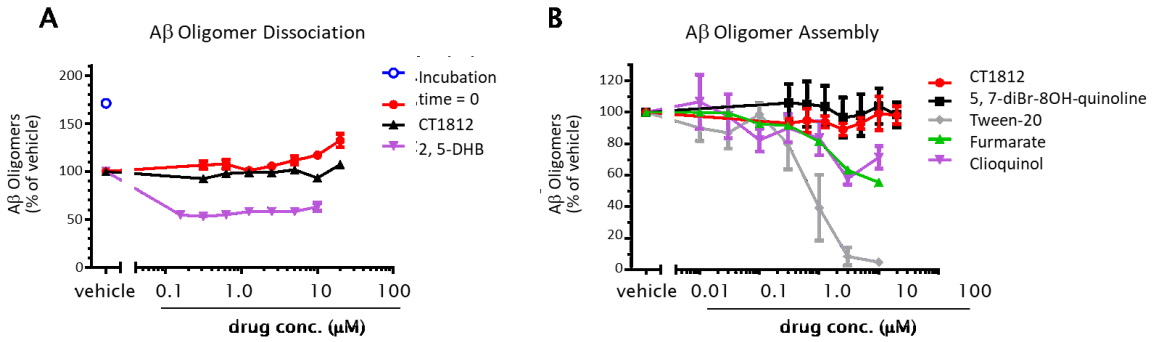

Supplementary Fig. 2. CT1812 reduction of Aβ oligomer presence is not reliant upon oligomer dissociation or inhibition of assembly. (**A**) One-site ELISA specific for oligomeric forms of Aβ 1-42. Preformed oligomers were incubated for 18 hours in the presence of increasing concentrations of compounds followed by assay for oligomeric Aβ remaining in solution. Aβ dissociates slowly over time on its own. The dissociation is enhanced by 2,5-Dihydroxybenzoic acid (2,5 DHB) [98] while Gallic acid stabilizes oligomers and prevents dissociation (data not shown). CT1812 (Fumarate salt) and a Na^{+}Fumarate control have no effect on dissociation. All values are normalized to 100% for vehicle control, except for the point for incubation time = 0, which represents starting oligomer concentration assayed before incubation. Error bars = SD. (**B**) Aβ 1-42 monomer was allowed to assemble into oligomers in the presence of increasing concentrations of compounds for 18 hours before being assayed for Aβ oligomers. Assembly of oligomers is inhibited by Tween20 [99], 5,7-diBr-8OH quinoline [100] but not by CT1812 or a Na^{+}Fumarate control. All data points represent mean ± SD of 3 replicates.

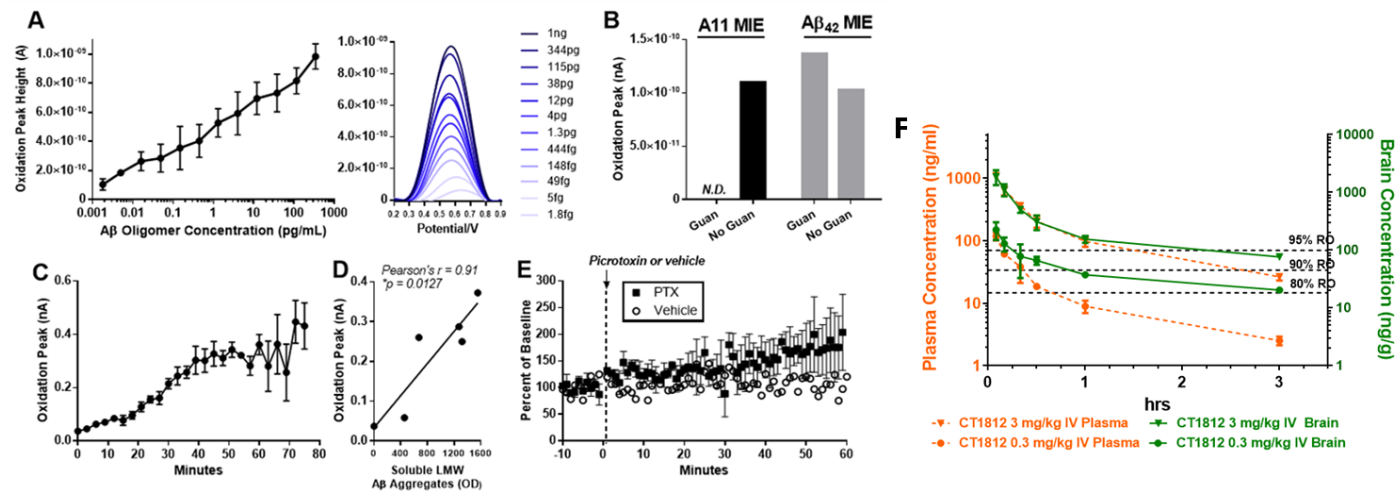

Supplementary Fig. 3. Microimmunoelectrode technology detects changes in Aβ oligomer concentration in CSF and brain. As previously published [40], this microimmunoelectrode (MIE) technology measures brain ISF levels of Aβ each minute in living 12 month old APP/PS1 mice. Microelectrodes can be coated with antibodies specific for Aβ40 monomer (HJ2) or oligomers (A11) and inserted into hippocampus to measure brain ISF Aβ levels or into lateral ventricles to measure CSF Aβ levels. (**A**) In vitro, Aβ aggregates as measured by A11 MIEs detect a robust signal in a solution of mixed $Aβ_{42}$ oligomers and fibrils but negligible signal in a solution of $Aβ_{42}$ monomer. (**B**) A11 MIE does not detect Aβ aggregates if guanidine is included to prevent their formation; however, the $Aβ_{42}$ MIE detects comparable levels of total $Aβ_{42}$ present. (**C**) A11 MIEs detect a rapid increase in signal as synthetic Aβ aggregates over 80 minutes at 37°C in vitro. (**D**) Signal on the MIE is tightly correlated with the levels of soluble aggregates over time as assessed by native-PAGE/western blot (Pearson's r= 0.91; p=0.0127). (**E**) In the brains of aged APP/PS1 mice, the A11 MIE detects a low level of Aβ aggregates at baseline, which increases gradually by 2-fold over 60 minutes following 30 mg/kg PTX-induced synaptic activity (n=4 per/group). (**F**) From previous PK studies in wild-type mice, a single i.v. dose of CT1812 (0.3 mg/kg, or 3.0 mg/kg; sigma-2 receptor Ki = 8.5 nM) results in a rapid rise in brain concentration that remains above 80% estimated receptor occupancy levels for >90 minutes. Horizontal lines mark concentrations of CT1812 equivalent to theoretical occupancy of the sigma-2 receptor of 80%, 90%, and 95% (4 x Ki, 9 x Ki, 19 x Ki, respectively).

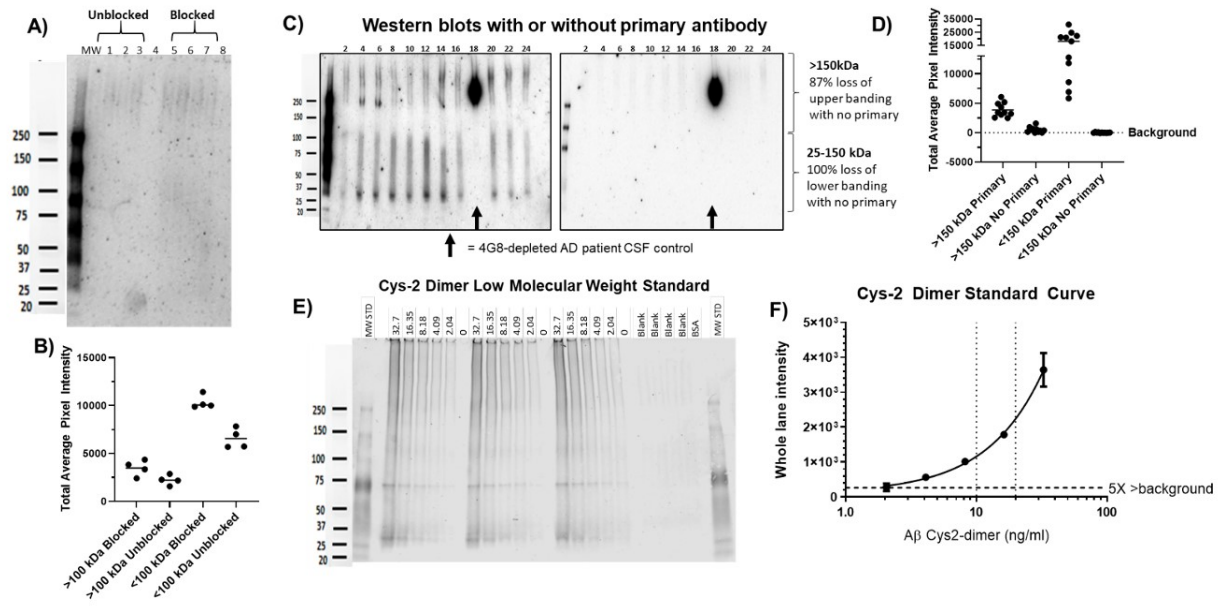

Supplementary Fig. 4. Validation of western blotting method for detection of Aβ oligomers. **(A-B)** Blocking tubes and plate wells via pretreatment with human serum albumin increases the recovery of Aβ oligomers [101]. CSF samples from one Alzheimer's patient (Discovery Life Sciences, USA) were thawed, transferred to microtiter plates that were either coated with 2% human serum albumin (HSA, isotonic with CSF) or left uncoated. The samples were then loaded onto 4 replicate gel lanes (lanes 6-9, albumin coated; lanes 1-4, uncoated; left most lane contains molecular weight standards [Precision Plus dual color standard, Bio-Rad Catalog #1610374]) and band intensity across the full length of the blot (loading lane to dye front) was quantified using the Alpha Innotech image system and Alpha View software (ProteinSimple, San Jose, CA). Compared to patient samples from unblocked wells, coating microtiter plates with HSA increased recovery of Aβ oligomers (high molecular weight (>100kD) 36% increase, low molecular weight (<100 kD) 37% increase). **(C-D)** Primary antibody, 82E1, specifically detects Aβ oligomers with a range of molecular weights. Alzheimer's patient CSF samples (Discovery Life Sciences) were loaded 1:1 with native sample buffer (Bio-Rad Laboratories, Hercules, California, USA; catalogue #1610738); each of these lanes contains a CSF sample from a different patient (left most lane contains molecular weight standards). Lane 18 (both blots) contains pooled Alzheimer's patient samples in which Aβ was depleted by a preincubation with 4G8 antibody prior to loading on gel. Blots were probed with (left) or without (right) 82E1 primary antibody (IBL America, Catalogue #10323) followed by Goat anti mouse IgG (H+L) HRP secondary antibody at 1:100,000 (10ng/ml, Millipore Catalog #AP308P), and band intensity across the full length of the blot (loading lane to dye front) was quantified. Aβ depleted patient samples (lane 18, left blot) have undetectable lower molecular weight species (size range 24-150kDa); upper molecular weight banding (>150kDa) is obscured by the large IgG signal. In the absence of 82E1 primary antibody (lane 18, right blot) lower banding (24-150kDa) is undetectable above background (100% lower in average intensity) and higher molecular weight species (>150kDa) are 87% lower in average intensity. **(E-F)** The sensitivity of this method for detecting Aβ oligomers in CSF is 2ng/mL (LLOQ, CV<20%). The Cys-2 dimer standard was diluted two-fold in AD patient CSF (32.7 ng/mL to 2.04 ng/mL, source: University of Gothenburg) and loaded in 3 replicate groups on the same gel (E). The left and right most lanes

contain molecular weight standards. Quantification of Aβ protein intensity (F) across the full molecular weight range (top of gel to dye front) reveals a lower limit of quantification (defined as 5x above background) of 2ng/mL (CV<20%). Two Cys-2 dimer concentrations in the middle of this sensitivity range (10 and 20 ng/mL, vertical dashed lines in E) were included as standards on each gel measuring patient samples. This method is sufficient for detecting relative changes in oligomer concentration in CSF above 2.5 ng/mL.

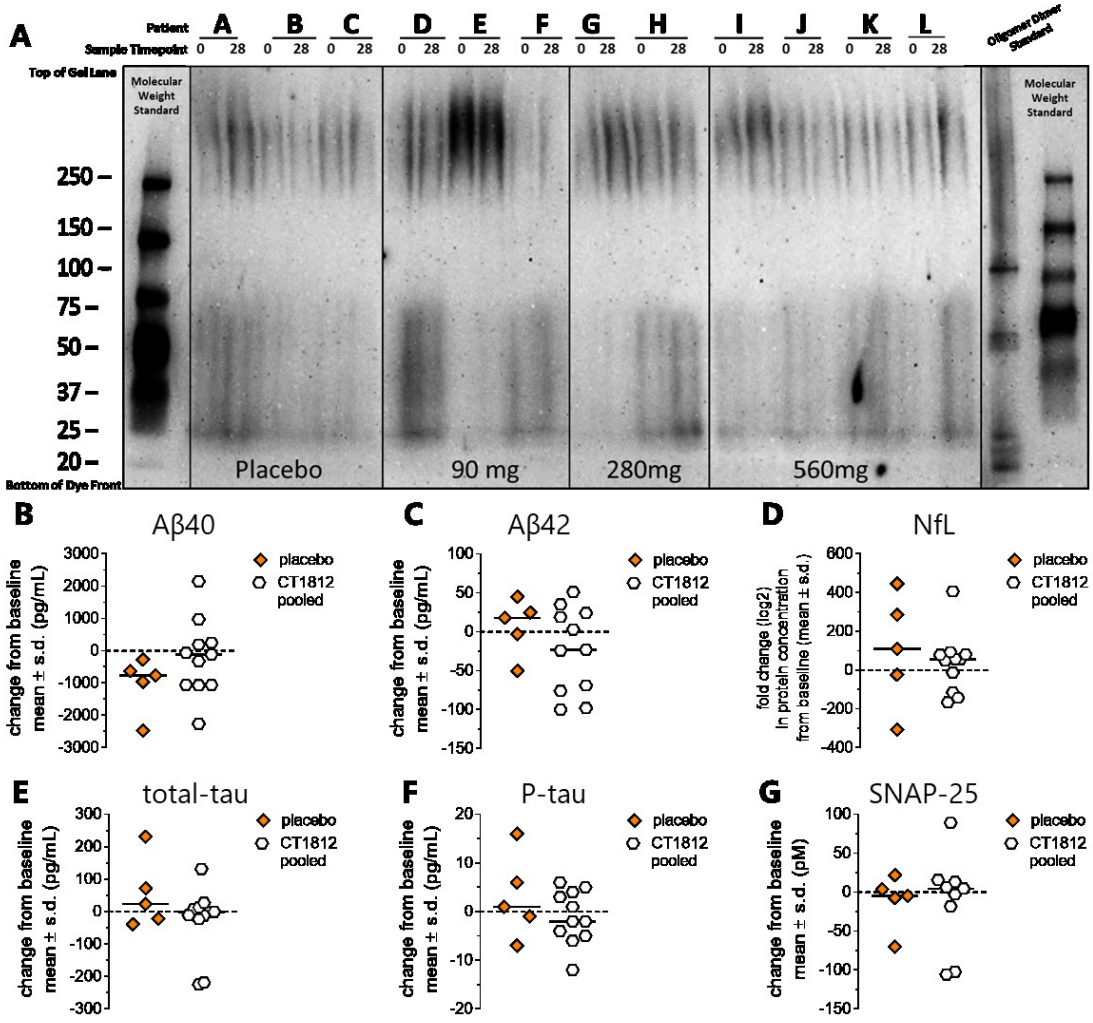

Supplementary Fig. 5. Western blot of Aβ oligomers in CSF of AD patients treated with CT1812 in clinical trial COG0102. (**A**) Aβ oligomer concentrations in CSF samples from AD patients in a 28 day phase 1b/2a clinical trial of CT1812 vs. placebo were measured via gel electrophoresis using non-denaturing conditions. Samples were run on Tris-HCl gels, transferred to nitrocellulose and probed with 82E1 mouse monoclonal Aβ antibody (IBL America, Minneapolis, MN) and visualized by chemiluminescence. Total intensity of the entire length of each lane was quantified using an Alpha Innotech image system. This composite image represents 12 of the 13 patients that were measured and analyzed to produce the results found in Figure 5A. (**B-G**) Mean change from baseline of targeted AD CSF biomarkers. None of the differences between placebo-treated and CT1812-treated patients were statistically different for these analytes.

A

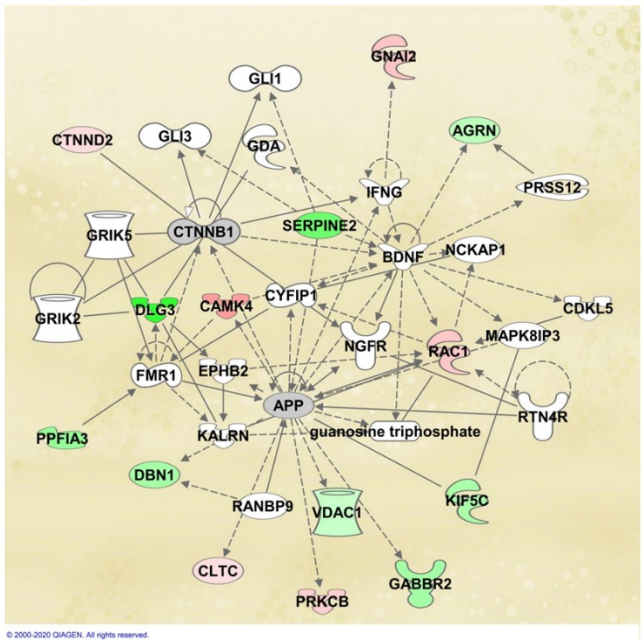

B

Diseases or Functions within Network	p-value
Dendritic growth/branching	9.91E-17
Branching of neurites	1.34E-16
Organization of cytoskeleton	5.68E-15
Synaptic transmission	5.93E-15
Neurotransmission	6.25E-15
Morphology of nervous system	8.13E-15
Development of neurons	2.47E-14
Microtubule dynamics	4.11E-14
Morphology of neurons	4.6E-14
Neuritogenesis	4.82E-14
Plasticity of synapse	1.58E-13
Morphology of central nervous system	3.64E-13
Formation of cellular protrusions	4.05E-13
Morphology of brain	1.25E-12
Proliferation of neuronal cells	2.22E-12
Abnormal morphology of central nervous system	2.82E-12
Proliferation of central nervous system cells	6.51E-12
Potentiation of synapse	7.48E-12
Quantity of neurons	8.59E-12
Abnormal morphology of brain	1.03E-11
Cognitive impairment	1.53E-11
Apoptosis of neurons	3E-11
Synaptic depression	3.56E-11
Length of neurons	4.92E-11
Abnormal morphology of neurons	5.24E-11

Supplementary Figure 6. Pathway analysis of synaptic proteins significantly altered in CSF of CT1812-treated patients vs. placebo. (**A**) To understand the subset of synaptic biology specifically impacted by CT1812 treatment, we performed pathway analysis (nervous system focused) with IPA comparing synaptic proteins that were significantly different between CT1812 and placebo patients (Fig 5 E, $p < 0.05$) to a Reference Set. The Reference Set was defined as the synaptic proteome specified in Lleó, et al, [102], further restricted to only the proteins detectable in the present COG0102 study CSF samples. The highest scoring Network was "Cell Morphology, Cellular Assembly and Organization, Cellular Development." Within this network, 14 out of 25 of the synaptic proteins were found, a number of proteins present that was a significantly greater than would be expected by random chance (IPA Score=26; $p < 1x10-25$). Levels of proteins shaded red were higher, whereas those shaded in green were lower in CSF from CT1812 (pooled) than placebo. (**B**) The top functions from this network include dendritic branching, cytoskeletal remodeling, and neurotransmission.

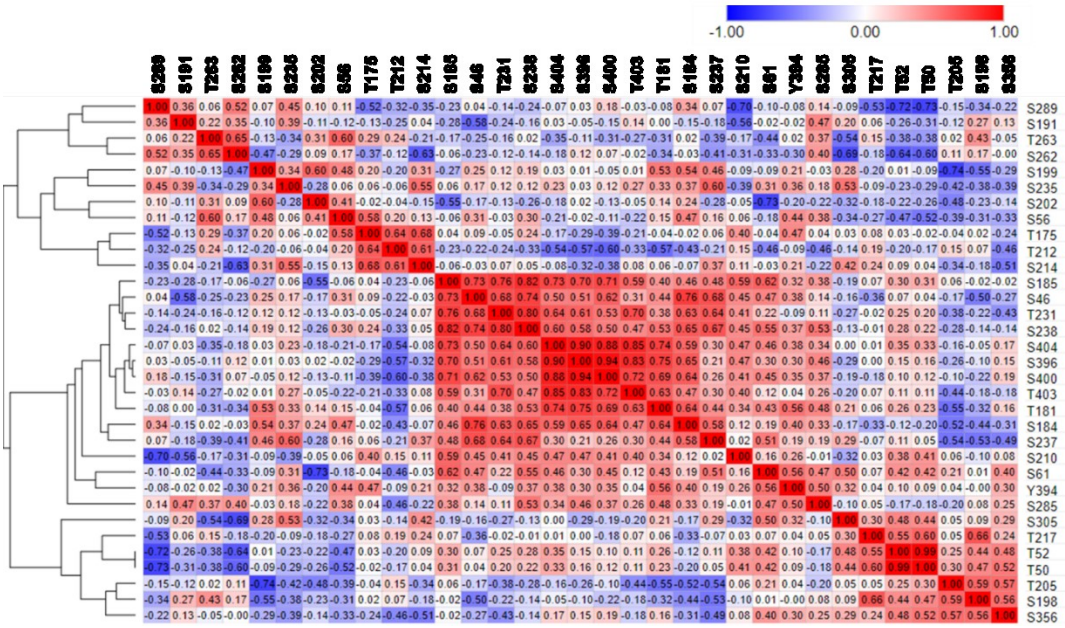

P-tau residue 1	P-tau residue 2	Correlation coefficient	p-value
S289	T50	-0.73	1.09E-02
S199	T205	-0.74	9.86E-03
S185	S238	0.82	2.01E-03
S185	T231	0.76	6.74E-03
S185	S404	0.73	1.16E-02
S185	S400	0.71	1.39E-02
S46	S184	0.76	6.74E-03
S46	S238	0.74	8.64E-03
S46	S185	0.73	1.08E-02
T231	S238	0.8	3.21E-03
S396	S400	0.94	2.16E-05
S396	S404	0.9	1.37E-04
S396	T403	0.83	1.52E-03
S400	S404	0.88	3.89E-04
S400	T403	0.72	1.17E-02
T403	S404	0.85	8.41E-04
T181	S396	0.75	7.99E-03
T181	S404	0.74	8.55E-03
S61	S202	-0.73	1.14E-02
T52	S289	-0.72	1.31E-02
T50	T52	0.99	2.65E-08

Supplementary Fig. 7. Inter-relationship of pTau sites in AD CSF from patients treated with CT1812. The change from baseline of each pTau site (in AD CSF) with all pTau sites was computed for all matched paired samples treated with drug (N=11) and Pearson correlation analysis was performed. (**A**) For visualization, a heatmap was generated using Pearson hierarchical clustering (Average Linkage, both rows and columns; https://software.broadinstitute.org/morpheus/). The color scale is a gradient reflecting the extent of association, with the highest positive correlation of 1 in dark red and highest negative correlation of -1 in dark blue. (**B**) Correlation coefficients and p-values for the 21 coregulated pairs of T-tau residues are shown. These results suggest that CT1812 may act upstream of tau kinases and phosphatases to impact tau phosphorylation at specific amino acid sites.